frontiers in Earth Science

ORIGINAL RESEARCH
published: 15 March 2022
doi: 10.3389/feart.2022.832104

Characteristics and Main Controlling Factors of Fractures within Highly-Evolved Marine Shale Reservoir in Strong Deformation Zone

Xuehui Zhou[1], Ruyue Wang[1]*, Zhili Du[2], Jing Wu[3], Zhonghu Wu[4], Wenlong Ding[5], Ang Li[6], Zikang Xiao[7], Zixian Cui[8] and Xinghua Wang[1]*

[1]SINOPEC Petroleum Exploration and Production Research Institute, Beijing, China, [2]Oil and Gas Survey, China Geological Survey, Beijing, China, [3]School of Earth Science and Engineering, Shandong University of Science and Technology, Qingdao, China, [4]College of Civil Engineering, Guizhou University, Guiyang, China, [5]School of Energy Resources, China University of Geosciences, Beijing, China, [6]College of Earth Sciences, Jilin University, Changchun, China, [7]National Institute of Natural Hazards, Ministry of Emergency Management of China, Beijing, China, [8]SINOPEC Star Petroleum Company, Beijing, China

OPEN ACCESS

Edited by:
Lei Gong,
Northeast Petroleum University, China

Reviewed by:
Kun Zhang,
Southwest Petroleum University, China
Shuheng Du,
Institute of Mechanics (CAS), China

***Correspondence:**
Xuehui Zhou
zhouxuehui.syky@sinopec.com
Ruyue Wang
wry1990@vip.qq.com

Specialty section:
This article was submitted to Structural Geology and Tectonics, a section of the journal Frontiers in Earth Science

Received: *09 December 2021*
Accepted: *31 January 2022*
Published: *15 March 2022*

Citation:
Zhou X, Wang R, Du Z, Wu J, Wu Z, Ding W, Li A, Xiao Z, Cui Z and Wang X (2022) Characteristics and Main Controlling Factors of Fractures within Highly-Evolved Marine Shale Reservoir in Strong Deformation Zone. Front. Earth Sci. 10:832104. doi: 10.3389/feart.2022.832104

Based on the systematical observations of cores, thin sections, and scanning electron microscope (SEM) sections, together with the testing data and characteristic parameters, this paper discussed the characteristics and controlling factors of fractures, and their control on shale gas accumulation in the Lower Cambrian Niutitang Formation black shale reservoir of Well YX1 in the northern Guizhou Province. The results show that macro structural fractures are common in the Niutitang Formation, which can be divided into shear fractures (e.g., high dip-angle shear fractures and low dip-angle slip fractures), tensional fractures, and tension-shear fractures. Non-structural fractures in microfractures can be divided into organic-related fractures and inorganic mineral-related fractures. Most of the structural fractures were filled and the types of fillings are diverse. The staggered relationships of fractures confirm the complexity of tectonic movement in the study area. The formation of structural fractures in Well YX1 is mainly controlled by the major fault. The influence of mineral composition and content, mechanical properties, brittleness, and organic matter content of rocks on the characteristics of the fractures are from the external manifestation of sedimentary environment. Affected by diagenetic evolution, organic matter-related fractures are not common. Compared with other shale gas reservoirs in China and abroad, the organic-rich shale reservoir of Well YX1 is characterized by both "geological sweet spots" and "engineering sweet spots"; however, strong deformation and faulting have led to the loss of shale gas and damage of the overpressure environment. Therefore, it is suggested that small-scale fractures, caused by tectonic movements but without large penetrating faults, are the most favorable for shale gas reservoirs. Based on the complicated tectonic setting in northern Guizhou, the formation pressure should be taken into account.

Keywords: structural fractures, non-structural fractures, micro-fractures, Niutitang formation, organic-rich shale

INTRODUCTION

Shale gas is a typical target that can be explored and developed in an industrialized manner under the current economic and technical conditions. The shale gas success in the United States (US) has especially changed the competitive landscape of the global natural gas market. In China, the organic-rich shales are widespread in strata of different geological ages, implying a great resource potential for prospective development. The presence of natural fractures is one of the key factors for the formation of a shale gas reservoir (Wang et al., 2018a; Gu et al., 2021; Xie et al., 2021). It plays a dual effect. On one hand, the presence of natural fractures decides directly the enrichment and production of shale gas. For the shales with low permeability and low porosity, the fractures can improve the seepage capacity of shale. In the brittle shale intervals with high elastic modulus, low Poisson's ratio, and rich organic matters, fractures are easily generated to facilitate the increase of free gas and desorption of adsorbed gas in shale formations (Ding et al., 2012). Well-developed fractures are favorable for shale gas reservoirs (Zeng W. T. et al., 2016; Wang et al., 2021). On the other hand, too large scale of fractures may lead to gas loss (Long et al., 2011; Zeng W. T. et al., 2016; Zeng L. et al., 2016; He et al., 2016). Multi-phase tectonic movements in the study area contributed to the abundance of structural fractures, which however are mostly filled by calcite and quartz. Related studies indicate that open fractures in shale would damage the sealing capacity of rocks, thereby hindering the occurrence of the overpressure environment which is conducive to gas accumulation (Li et al., 2016). However, the fractures sealed by cements may prevent further gas loss, which is relatively favorable to the preservation of shale gas. Moreover, the sealed fractures, which damage the integrity of shale strata and form weak zones, may make induced fractures extending in a single direction diverge into more directions, so as to improve the stimulation performance (Weng et al., 2011; Cho et al., 2013; Gale et al., 2014; Li et al., 2015).

The study on reservoir fractures began in the mid-20th century. By far, the study methods have changed from qualitative description to quantitative research, and the reservoir fracture identification technologies have evolved into a multidimensional system comprised of points (cores and thin sections), lines (well logging data), surfaces (outcrops), bodies (seismic data) and time (production dynamic data) (Ding et al., 2012; Hou and Pan, 2013; Lang et al., 2014; Kosari et al., 2015; Moumni et al., 2016; Bisdom et al., 2017; Han et al., 2019; Zhong et al., 2021). The study on micro-fractures in shale flourished along with the exploitation of shale oil and gas, by means of observations using scanning electron microscope (SEM) (ca. 1960), cold cathodoluminescence microscope (CCLM) (Sipple, 1968) and SEM-based cathodoluminescence microscope (CLM) (Pagel et al., 2000; Gomez and Laubach, 2006). Researchers have proposed some classification schemes for micro-fractures. Typically, the micro-fractures were classified by (1) geological origin; structural fractures and non-structural fractures which are subdivided into diagenetic shrinkage fractures, pressolutional stylolites, overpressure fractures (e.g., undercompaction-induced overpressure fractures, hydrocarbon generation-induced overpressure fractures, and HP crushing-induced fractures); thermal shrinkage fractures; dissolution fractures; and weathering fractures (Long et al., 2011; Guo et al., 2014; Pu et al., 2014; Zhang et al., 2014; Wang J. L. et al., 2015; Yuan et al., 2015; Ma et al., 2016; Yuan et al., 2016); (2) position and matrix relationship, interlayer fractures, matrix mineral related fractures, clay mineral related fractures, and organic-related fractures which could be subdivided into intergranular and intragranular fractures (Yang et al., 2013; Liu Y. X. et al., 2015); (3) size of fractures (Wang Y. et al., 2015); and (4) the combination of the above-mentioned methods (Ye et al., 2012; Zhang et al., 2014; Clarkson et al., 2016; Yu et al., 2016; Zhang et al., 2016a).

The content of brittle minerals is also one of the influential factors for shale fractures. There are many brittleness characterization methods based on minerals, such as quartz (Kassis and Sondergeld, 2010), quartz and dolomite (Slatt and Abousleiman, 2011), feldspar and dolomite (in addition to quartz) (Nelson, 1985), and quartz, feldspar and carbonate minerals (e.g., calcite) (Du et al., 2011). Diao (2013) combined the mineral composition method and the rock mechanics method for calculating brittleness index. Zhang et al. (2016a) suggested quartz, dolomite, and pyrite as brittle minerals for brittleness calculation.

In the northern Guizhou Province located in the hinterland of Southwest China, there are two sets of organic-rich black shales in the Lower Paleozoic, i.e., the Lower Cambrian Niutitang Formation and the Lower Silurian Longmaxi Formation. These shale formations are characterized by huge sedimentary thickness, extensive lateral extent, high TOC content, and a relatively high degree of thermal maturation with moderate burial depth, showing great hydrocarbon generation potential. However, they have not been efficiently ascertained with regard to accumulation conditions, enrichment mechanism, and favorable zone distribution due to the complexities in geological setting, sedimentary environment, and tectonic conditions in South China. The main objectives of this paper are to analyze rock mineral composition, petrographic thin sections, TOC, and SEM data to (1) characterize the types and characteristics of fractures, (2) analyze the key factors for the different types of fractures, and (3) determine faults and fractures control on shale gas accumulation.

GEOLOGICAL SETTING

The Well YX1 is located in the Northern Guizhou Province (**Figure 1A**) which is generally a part of the Yangtze block and adjacent to the North China block, South China fold belt, and Qinghai-Tibet plate (**Figure 1B**). The tectonic evolution of the Fenggang-1 area is consistent with the regional tectonic evolution in northern Guizhou Province. The northern Guizhou Province has experienced two tectonic and sedimentary evolution stages: The first is the Caledonian-Hercynian period, where the tectonic movements are mainly dominated by tectonic fluctuation and tension, accompanied by intermittent compression, which

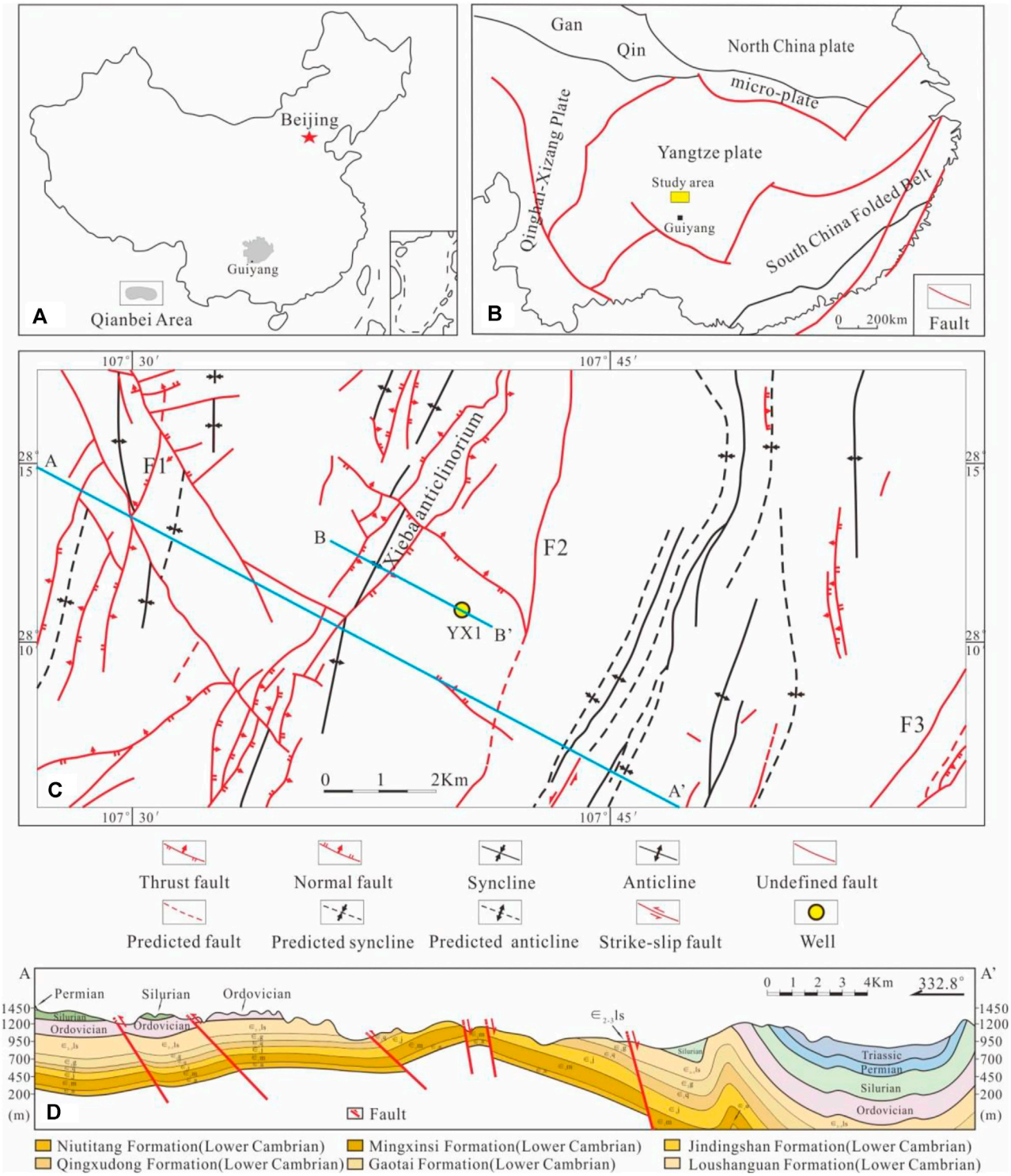

FIGURE1 | (A) Location of the Qianbei Area; **(B)** Location of the Yangtze plate tectonic unit with the studying area in the south of the Yangtze plate; **(C)** Fracture system of the study area and the well location; **(D)** a NW-SE trending, structural section with the location shown in **(C)**. And the BB′ is the location of YX1 well offset time profile of **Figure 10**.

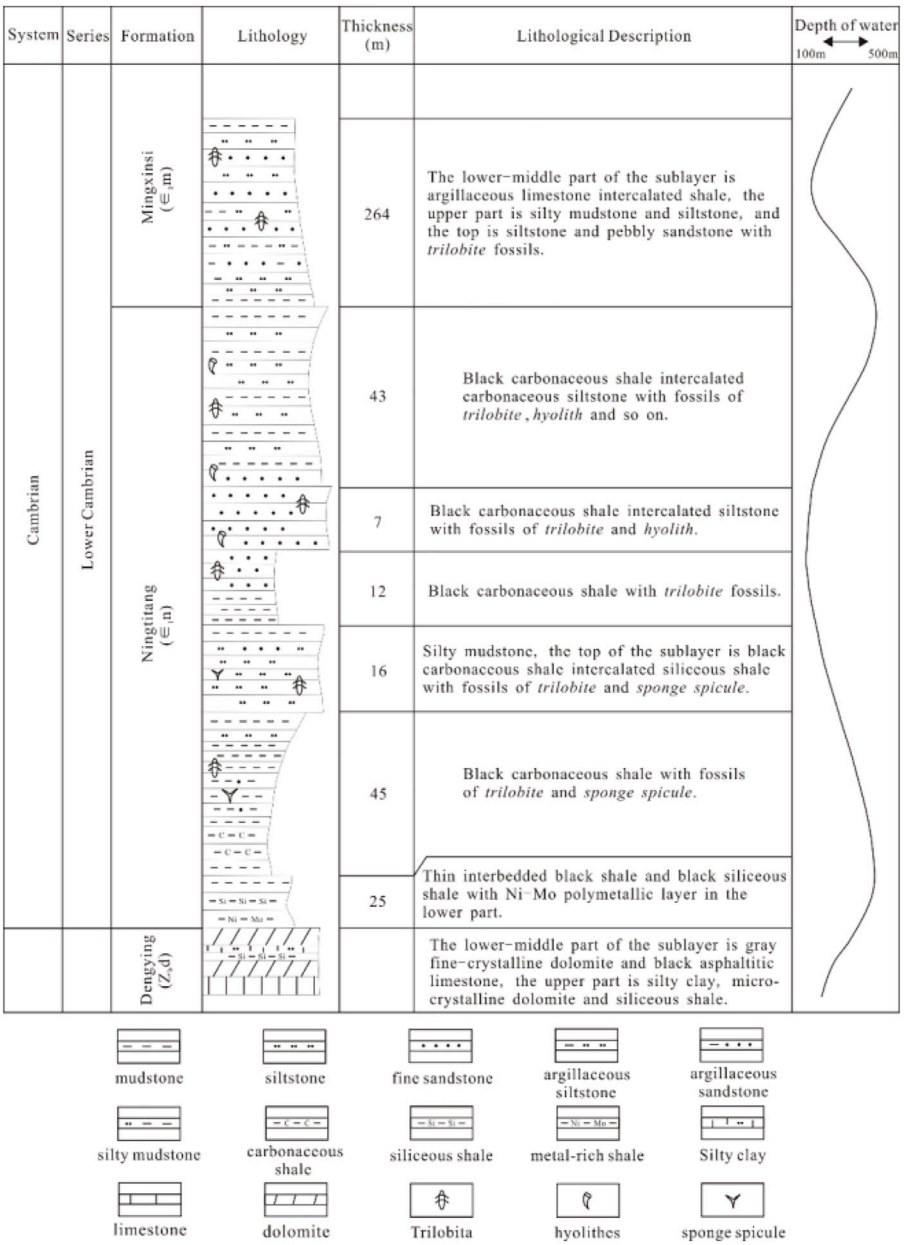

FIGURE 2 | Comprehensive stratigraphic column of the Niutitang Formation in Lower Cambrian of Guizhou Province (Modified by China's Stratigraphic Editorial Board, 2009).

formed a structural framework of alternative uplift and depression regionally and deposited sedimentary buildings dominated by marine carbonate rocks intercalated with clastic rocks, The second is the Indosinian and later stage. Due to continental collisions started in the Middle-Late Triassic period, tectonic transformation occurred in the study area from tension due to compression and developed a continental sedimentary system. Due to the compressional stress in the southeastern part during the late Yanshan-Himalayan period, the area was dominated by uplifting, folding, and the deposition area was gradually reduced. Northern Guizhou Province is subject to strong SE-NW compressional stress (Jiu, 2014).

This zone is dominated by compressional deformation, as well as strike-slip features. The long-term interference and superposition of structures developed in different periods shaped the present structural framework characterized by folds and faults in complex configurations. Moreover, there are trough-like folds with tightly-closed synclines and wide, gentle anticlines. The Permian and Triassic strata are mainly preserved in the syncline core, and the Cambrian and Ordovician strata in the

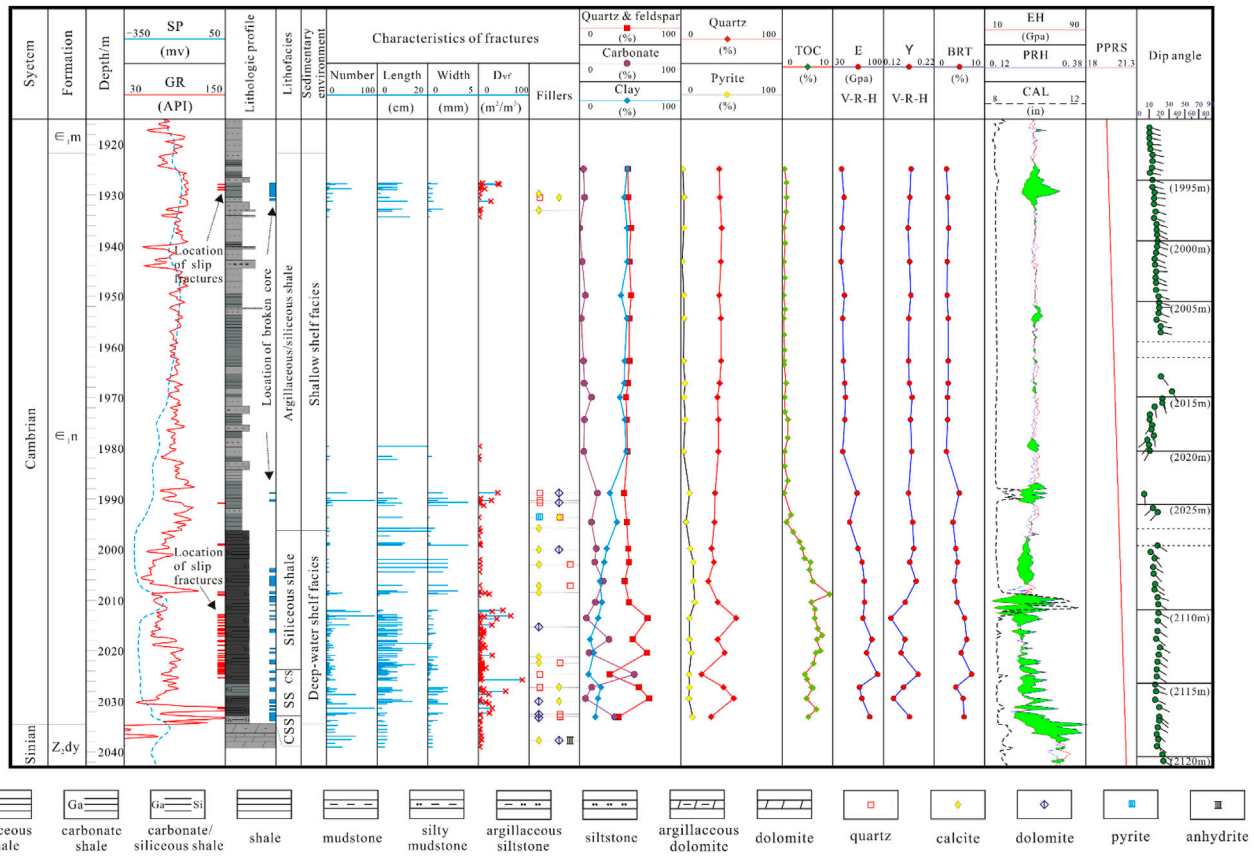

FIGURE 3 | The comprehensive column of the characteristics of shale fracture development in the Niutitang Formation of Well YX1. BRT represents brittleness index, EH represents dynamic Young's modulus, PRH represents dynamic Poisson's ratio, PPRS represents pore pressure and Dvf represents volume density of fractures.

anticline core (**Figures 1C,D**). The Lower Cambrian Niutitang Formation in the study area generally consists of black carbonaceous shale, siliceous shale, mudstone, silty mudstone, and argillaceous siltstone etc., with common fossils such as trilobites, hyolithes, and sponge spicules (**Figure 2**).

The target formation of Well YX1, the Niutitang Formation (ϵ_1n, 1921.7–2034.5 m), is a set of deposits of deep continental shelf–shallow continental shelf facies (**Figure 3**). Its bottom (2007–2034.5 m) is dominated by black siliceous shale with a large amount of high resistivity fractures as well as pyrites distributing along the formation. Upwardly, the lithology transits to argillaceous siliceous shale and silicon-rich argillaceous shale due to the gradual increase of shale content, with much less pyrite content (1996.5–2007 m). Its middle-upper part (1921.7–1996.5 m) is dominated by silty mudstone, with dark grey argillaceous siltstone locally, and rare pyrite. Its lower part (1996.5–2034.5 m) has an organic content (TOC of 2.17–9.36% or 5.8% on average, mainly Type II_1), suggesting a set of self-generation and self-preservation shale gas reservoirs. According to the analysis of the core data, the Niutitang Formation of Well YX1 has a porosity of 0.85–4.51% (2.23% on average) and a permeability of $(0.0031–0.0125)\times10^{-3}$ μm^2 (0.0064×10^{-3} μm^2 on average), presenting as a low-porosity and low-permeability reservoir.

SAMPLES AND METHODS

Shale Sample Tests

Shale core samples were taken from the Niutitang Formation of Well YX1 for whole rock and clay mineral X-ray diffraction analysis (24 samples), TOC test (52 samples), SEM analysis (24 samples) and thin section observations (18 samples).

The whole rock and clay minerals X-ray diffraction analysis was conducted with the Panalytical X 'Pert PRO MPD multi-functional X-ray diffraction analyzer under the temperature of 24°C and the environmental humidity of 35% in Beijing Research Institute of Uranium Geology. The samples were exposed in Cu-K_α X-ray with characteristic wavelength of 1.5418Å after oil washing, drying, and grinding and then scanned at the rate of 4°/min within the range of 3–85° (2θ) to obtain the diffraction data. The relative mass percentages of minerals were determined by the semi-quantitative method using the peak area of each mineral in the diffraction data curves obtained, and then

corrected for Lorentz Polarization (Pecharsky and Zavalij, 2003). Based on the X-ray diffraction data, the sedimentary background, diagenetic evolution stage, and rock mechanics characteristics of the fractured formation are studied.

The TOC test was completed under the room temperature of 25°C and the environmental humidity of about 60% in Geochemical Experiment Center of Yangtze University. The samples were stripped of inorganic carbon by using the diluted hydrochloric acid with V_{HCl}: V_{H2O} of 1:7, and then burned in a high-temperature oxygen stream to convert total organic carbon to CO_2. Finally, the TOC was determined using the LECO CS230 carbon-sulfur analyzer. Based on the TOC data, the sedimentary background and the influence of TOC content on fractures are studied.

The field emission scanning electron microscope (FESEM) analysis was performed in China University of Geosciences (Beijing). The samples were ground into sections in 1 cm × 1.2 cm and polished by argon ion, with the 10–20 nm thick gold films applied on the polished surface to increase the electrical conductivity. Then, the samples were observed using the Zeiss SUPPA55 FESEM. Based on the FESEM data, the microfractures and sedimentary background are studied.

Representative samples with different fracture fillings were selected from the core sections and then ground into thin sections of 2 cm × 2 cm. Then, the types, geometry, and intersection of such fillings were observed under the OLYMPUS Polarization Microscope.

Fracture Description Method

(1) In this study, macroscopic and non-structural fractures and filling characteristics of fractures in YX1 well were introduced. Microscopic fractures are mainly studied for non-structural fractures. From the tectonic setting, depositional, and diagenetic evolutions, the factors influencing the development of fractures were analyzed. Finally, the effects of fault and fracture on shale gas preservation were analyzed.
(2) A brief introduction to the V-R-H model is used in Section 5.3.2.

Voigt (1910) proposed an equal strain averaging model on the assumption that all components have the same strain:

$$M_V = \sum_{i=1}^{N} f_i M_i$$

Where M_V——The elastic modulus of mixed media in Voight model; f_i——The volume fraction of the i-th medium; M_i——The elastic modulus of the i-th medium.

Reuss and Angew (1929) proposed an equal stress averaging model on the assumption of the same stress for each component:

$$\frac{1}{M_R} = \sum_{i=1}^{N} \frac{f_i}{M_i}$$

Where M_R——The elastic modulus of mixed media in Reuss model; the meanings of fi and Mi are the same as those of the Voight model.

Hill (1952) established the Hill model. In the V-R-H model, the Voigt Model and Reuss model represent the upper and lower bounds of the values of elastic modulus and Poisson's ratio, and the V-R-H model represents the mean of both parameters. The V-R-H model can significantly improve the accuracy of the estimation results.

$$M_{VRH} = \frac{M_V + M_R}{2}$$

RESULTS

Lithofacies and Mineral Composition

Lithofacies

Based on the whole rock X-ray diffraction analysis results and TOC content, and according to the lithofacies classification by "three end members of rock minerals + sedimentary microfacies" proposed by Wang Y. F. et al. (2016), two typical lithofacies combinations were identified in the Niutitang Formation (**Figure 4A**), i.e., deep continental shelf facies combination (Wang R. Y. et al., 2016b) and shallow continental shelf facies combination (Wang R. Y. et al., 2016b). The former (2.17% < TOC<9.36%) includes siliceous shale (SS) facies, calcareous-siliceous shale (CSS) facies, and calcareous shale (CS) facies, revealing a high abundance of organic matters. The latter (0.29% < TOC<1.14%) includes clay-siliceous shale facies with poor organic matters.

Rock Minerals

The whole rock and clay X-ray diffraction analysis result of 24 samples show that the minerals vary in the whole formation, with quartz and illite (a clay mineral) recording the highest content, followed by plagioclase, dolomite, and pyrite (**Figure 5**). All minerals in target intervals were divided into three types (clay, quartz–feldspar–pyrite, and carbonate), and mapped to a mineral triangle (**Figure 4B**). According to comprehensive analysis, in view of clay, which is dominated by illite and chlorite, the clay content ranges between 8.7% and 47.1% with an average of 31.5%, and reduces gradually from shallow layer to deep layer, showing plasticity in the shale. In view of quartz–feldspar–pyrite, which is dominated by plagioclase, the quartz–feldspar–pyrite content ranges between 37.4% and 76.7% with an average of 56.1%, and it is generally lower in the lower part than that in the upper part These types of minerals are commonly believed to be brittle which is conducive to fracture generation. In view of carbonate, the carbonate content varies greatly between 0.0% and 54.0%, with an average of 12.4%, and it increases gradually from shallow layer to deep layer; especially as the dolomite content increases rapidly. This set of organic-rich shale has similar mineral composition and brittle minerals content to the Barnett shale and Woodford shale in the US.

Fractures

Fracture Types

Core observation and description reveal the presence of complex fractures in the Niutitang Formation of Well YX1. These fractures

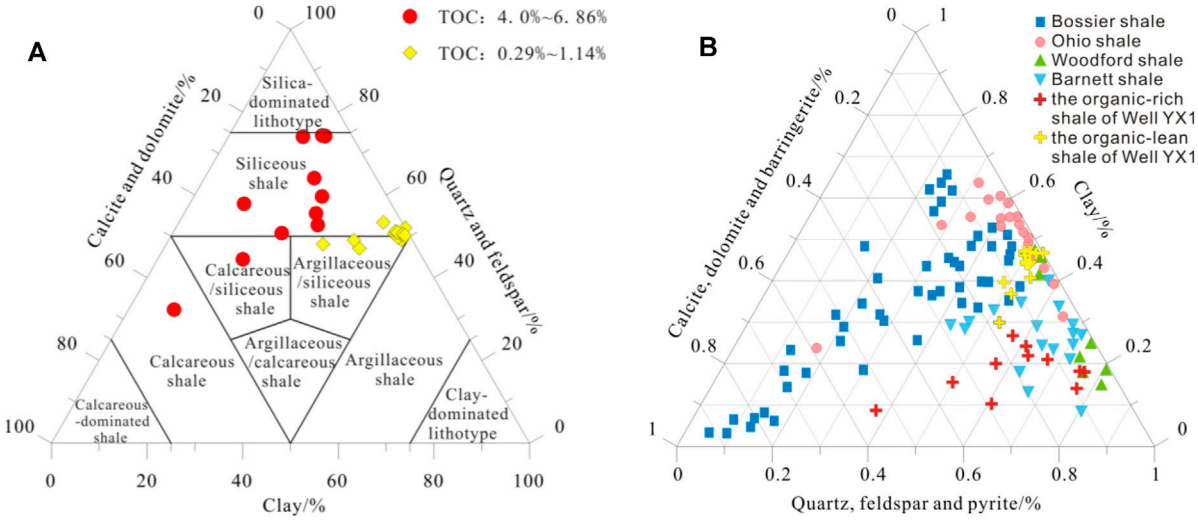

FIGURE 4 | (A) The lithofacies ternary diagram of the Niutitang shale of Well YX1; **(B)** Mineralogical ternary diagram of shales.

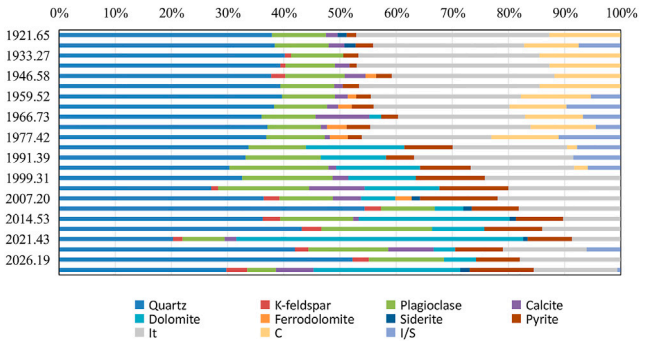

FIGURE 5 | The mineral composition of the Niutitang shale of Well YX1.

are divided into structural fractures and non-structural fractures by geological origin (Ding, 2015). In this classification, all fractures related to structural processes are classified as structural fractures. The structural fractures in this study area, which are the most abundant, are subdivided into shear fractures, extensional fractures, and tensional-shear fractures (**Figure 6**) (Liu et al., 2008). The non-structural fractures mainly include bedding fractures and overpressure fractures (Ding, 2015; Yuan et al., 2016).

Types and characteristics of structural fractures in the study area are described as follows.

Shear Fractures

The shear fractures are dominated by vertical or high dip-angle structural fractures, with long extension and straight fracture surface, or an occasional shear-sliding-induced striation. They are often developed directionally in groups and mostly filled. The shear fractures in Well YX1 are long, up to 2.58 m (**Figures 6A,B**). Slip fractures, another common type of shear fractures in the study area, have small dip angles, and generally occur in the horizontal direction or in a low dip-angle. Such fractures result from shearing along the weak mudstone formations under tectonic compression or extension (Zeng et al., 2007), with striation and mirror features on fracture surfaces (**Figures 6C,D**).

Extensional Fractures

The extensional fractures are characterized by unstable occurrence and short extension. Single extensional fractures are short and slightly curvy. The fracture surfaces are rough, without striation. The extensional fractures in the study area are mostly irregularly dendritic or net-shaped and filled (**Figures 6E,F**).

Tensional-Shear Fractures

Compared with high dip-angle shear fractures, the tensional-shear fractures have greatly varied fracture surface flatness, dip angle, and openness. Some main fractures may be associated with small branch fractures. Similarly, the tensional-shear fractures are developed directionally in groups and mostly filled by calcite (**Figure 6G**).

In addition, the serrated extensional fractures formed by traceable X-conjugate shear joint were detected in the study area (**Figures 6H,I**). Generally, different types and periods of fractures often appear in combinations (**Figures 6I,J**), reflecting the complex tectonic setting in the study area.

Types and characteristics of non-structural fractures in the study area are described as follows.

Bedding Fractures

As the most common type, the diagenetic bedding fractures are usually represented by horizontal fractures (**Figure 6K**). They are the product of under alternating hydrodynamic conditions (strong and weak), and easy to split due to their weak mechanics (Long et al., 2011). The bedding fractures act as favorable reservoir space, and are also main flowing channels

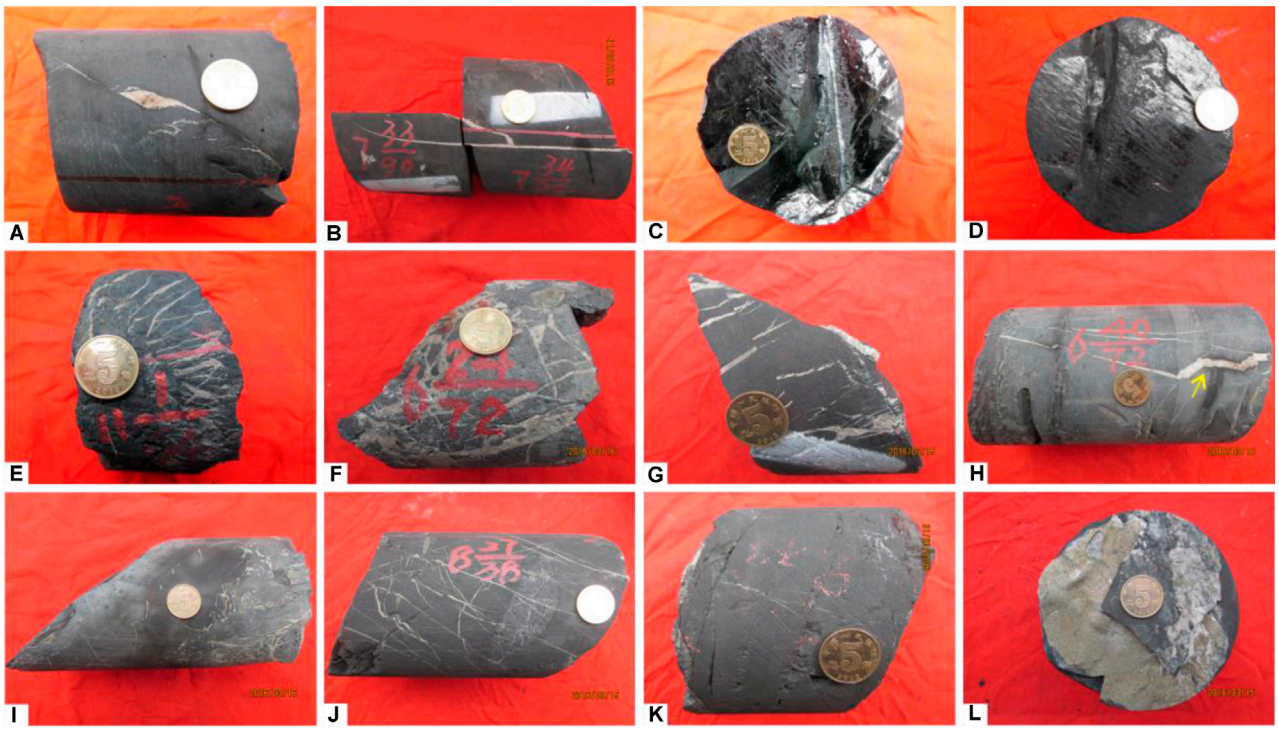

FIGURE 6 | Fractures in the cores of the Niutitang shale of Well YX1. **(A)** 2019.4 m, high dip-angle shear fracture with the small-sized rhombic block filled by calcite; **(B)** 1998.25–2000.83 m, calcite -filled vertical shear fractures of 258 cm long and 1–3 mm wide; **(C)** 2024.7 m, low dip-angle slip fracture with scratches and steps developed; **(D)** 2019.3 m, horizontal slip fracture with a smooth mirror; **(E)** 2022.6 m, branched-shaped extensional fractures filled by calcite; **(F)** 1985.6 m, network extensional fractures filled by calcite; **(G)** 2006.0 m, parallelly arranged tensional-shear fractures with small branches and filled by calcite, the tensional-shear fractures were split by the slip fracture; **(H)** 1988. m, Jagged and calcite-filled tensional-shear fractures formed by tracking the X-type conjugate shear joints; **(I)** 1987.0 m, Jagged and calcite-filled tensional-shear fractures formed by tracking the X-type conjugate shear joints. The left side of the core has low dip-angle slip fracture; the right side was crushed and filled by calcite. **(J)** 2012.0 m, network fractures were formed by the conjugate shear fractures and the low dip-angle fractures associated with extensional fractures. The narrow fractures were filled with calcite, and the larger fractures were filled with calcite and quartz. **(K)** 2010.2 m, diagenetic bedding fractures; **(L)** 2004.0 m, overpressure fracture filled by pyrite, fibrous calcite and quartz.

for shale reservoir fluids, being conducive to improve the reservoir preservation and seepage capacities (Hu et al., 2014).

Overpressure Fractures

Hydrocarbon generation, the expulsion of the organic-rich shale in certain conditions, or the formation of abnormal pore fluid pressure in the thick shale during a rapid burial stage, as well as other factors, might give rise to overpressure fractures (Kobchenko et al., 2011; Yuan et al., 2016). The overpressure fractures are generally irregular, not in groups, and often filled by calcite, pyrite, or quartz occasionally (**Figure 6L**). Antitaxial fibrous calcite veins, containing hydrocarbon inclusions, and parallel to shale bedding in shaly source rocks, (**Figures 7D,E**) can serve as markers for hydrocarbon expulsion and migration under abnormal high pressure within the petroliferous basin, and are also important evidence of hydrocarbon generation in shaly source rocks and primary migration of hydrocarbons (Wang M. et al., 2015). In addition, when the pore fluid pressure in the overpressure system is greater than the tensile strength of the sediments, vertical fractures can also be formed (Bour and Lerche, 1994).

As shown in **Figure 3** and **Table 1**, fractures are mainly developed in the upper part (1988.5–2034.21 m) and the lower-middle part (1926.5–1935.5 m). The lower part (2011.5–2034.2 m) contains more fractures than the upper and lower-middle parts (1988.5–2009.5 m). According to the statistics of structural fractures in shale core samples (**Figure 8**), the structural fractures are dominated by high dip-angle and vertical fractures and horizontal fractures are mostly slip fractures (**Figure 8A**). The fracture length ranges between 0 and 5 cm, followed by 5–10 cm (**Figure 8B**). The fractures with aperture ≤1.0 mm are overwhelming (**Figure 8C**). In view of filling, 93.4% of the fractures are filled and the unfilled fractures are mostly low dip-angle slip fractures. These characteristics are similar to those of fractures in shale gas wells in the southeastern Chongqing–northern Guizhou region, South China (Wang R. Y. et al., 2016a). The imaging logging data suggest the dominance of high resistivity fractures, high conductivity fractures, and small faults in Well YX1. High-resistivity fractures are not completely filled with high-resistivity minerals such as calcite, and they rather have a certain aperture, belonging to effective fractures. Fracture gaps are nearly or completely filled with igh-resistivity minerals

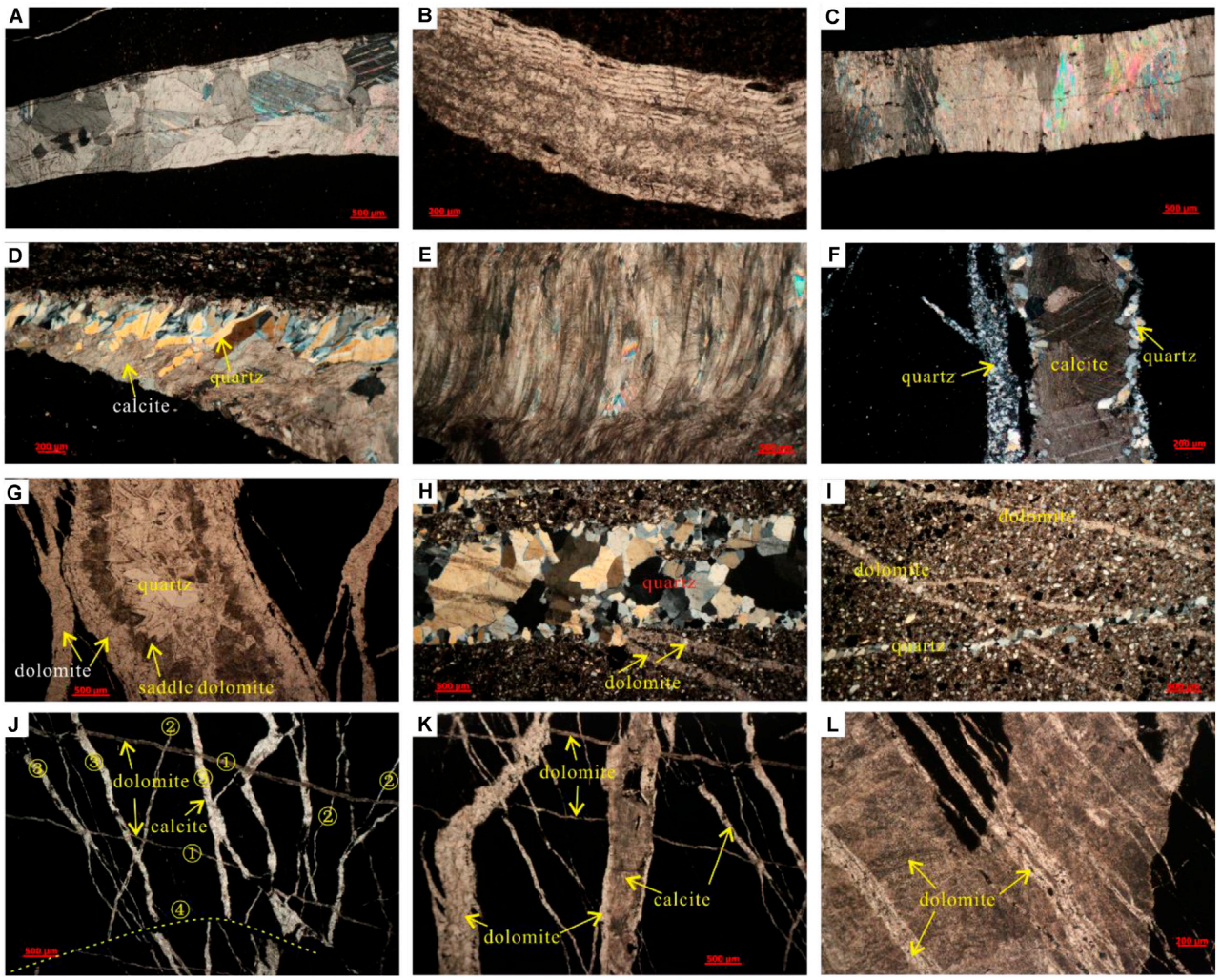

FIGURE 7 | Micrographs of the fracture fillers of Niutitang shale. **(A)** 1926.53 m, syntaxial blocky calcite vein, the calcite vein with better crystal status has the characteristics of multistage growth, orthogonal light; **(B)** 1929.77 m, calcite-filled fracture, the calcite vein with poor crystal status has the characteristics of multistage growth, plainlight; **(C)** 1999.76 m, syntaxial stretching calcite vein with the characteristics of multistage growth, orthogonal light; **(D)** 1990.46 m, antitaxial fibrous calcite- and quartz-filled fracture with the competitive growth of calcite and quartz, orthogonal light; **(E)** 2003.94 m, antitaxial fibrous calcite-filled fracture, the bending of the fibers was formed by progressive deformation of the crystal growth, orthogonal light; **(F)** 2024.05 m, fractures were first filled with calcite and later converted by hydrothermal quartz, orthogonal light; **(G)** 2029.8 m, fractures were first filled with calcite and later converted by hydrothermal quartz. The dolomite in contact with the quartz has the typical characteristics of saddle dolomite, plainlight; **(H,I)** 1987.52 m, the quartz-filled fractures formed in the early stage and the later formed the dolomite-filled fractures, orthogonal light; **(J,K)** 2026.81 m, there are four stages of fractures, followed by dolomite-filled low dip-angle fractures, dolomite-filled or dolomite/calcite filled rightward dipping fractures, calcite-filled leftward dipping fractures and slip fractures, plainlight; **(L)** 2029.8 m, two stages of dolomite-filled fractures, plainlight.

(calcite), showing poor effectiveness. The high resistivity fractures strike in nearly NS with the dip angle of 52° (**Figures 8E,H**), and are mainly distributed between 2014.0 and 2030.5 m, which is consistent with the core observation results. The high conductivity fractures and micro-faults mainly strike in NNE-SSW (**Figures 8D,F**), with the dip angle of 58° (**Figure 8G**) in dominance and between 14° and 78° (**Figure 8I**), respectively. The high conductivity fractures, micro-faults, and high resistivity fractures are all moderate—high dip-angle fractures in terms of occurrence. The high conductivity fractures are mainly distributed in 1927–1930 m, with low dip-angle, and the high dip-angle unfilled fractures with a length of 0.5 m or more are also observed, which is consistent with the core observations in this interval (**Figure 8**).

Fracture Cement

Fractures in the Niutitang Formation shale reservoir of Well YX1 show variable features under the microscope. They vary greatly in shapes and intersect in multiple manners. The fillings are diverse in type and variable in contact relationships. **Figures 7A–C** show the fractures filled by calcite, which grew in multiple periods and are different in crystal form. **Figure 7D** shows the fractures filled

TABLE 1 | Comparison of the mean values of fractures developed and undeveloped.

Top(m)	Bot (m)	Quartz (%)	Potash feldspar (%)	Plagioclase (%)	Calcite (%)	Dolomite (%)	Siderite (%)	Ankerite (%)	Pyrite (%)	Clay (%)	TOC(%)	BRI (%)	E (GPa)	ϒ	Evaluation
1926.5	1936.0	38.4	0.0	9.6	2.8	0.0	2.0	0.0	3.1	44.1	0.8	41.5	45.6	0.17	Developed
1936.0	1988.0	38.3	0.4	9.6	2.6	0.2	0.3	1.1	2.8	44.7	0.5	41.4	44.7	0.17	Undeveloped
1988.0	2007.0	31.4	0.2	14.7	2.8	13.9	0.0	0.0	9.4	27.5	3.4	54.7	65.1	0.18	Developed
2007.0	2034.5	39.4	2.9	11.5	2.9	16.8	0.8	0.4	9.6	16.0	6.4	65.7	77.0	0.16	Well developed

by fibrous calcite and quartz, which present obvious competent growth. **Figure 7E** shows the fractures filled by fibrous calcite or fibrous quartz occasionally. The fibrous waviness shown in **Figures 7D,E** resulted from the progressive deformation during the crystal growth (Durney and Ramsay, 1973; Ramsay, 1980). **Figure 7F** shows the fractures with small aperture and filled by quartz and the fractures with large aperture and filled by quartz-surrounded calcite. The latter is supposed forming due to the late hydrothermal transformation of quartz. **Figure 7G** shows the fractures filled by quartz in the center, indicating saddle dolomite adjacent to the quartz and fine-crystalline dolomite at the periphery. The saddle dolomite is an important indicator for hydrothermal transformation (Xu, 2009), suggesting that such fractures were attributed to the early dolomite filling and the late hydrothermal transformation of quartz. **Figures 7H,I** show the quartz-filled fractures and dolomite-filled fractures, with the former appearing earlier. **Figures 7J,K** reveal four stages of fractures, including low dip-angle dolomite-filled factures which were formed the earliest, right-dipping dolomite-filled or dolomite surrounded calcite-filled fractures, left-dipping calcite-filled fractures, and strike-slip fractures which break the first three stages of fracture. **Figure 7L** presents two stages of dolomite-filled fractures. All these characteristics of micro-fractures clarify the complex tectonic setting of this area.

On the whole core section, fracture fillings of the Niutitang Formation of Well YX1 are dominantly quartz and calcite in the upper part, and calcite, quartz and dolomite in the middle-lower part, followed by pyrite or anhydrite occasionally.

Micro Non-structural Fractures

Fractures having apertures of less than 0.1 mm are termed "microfractures" (Laubach, 2003; Anders et al., 2014). Based on the SEM data, micro-fractures in the Niutitang Formation of Well YX1 are found as structural and non-structural, here focusing on non-structural fractures. According to the classification proposed by Yang et al. (2013), the non-structural fractures are divided into organic matter related fractures (e.g., fractures around the organic matter edge and fractures within the organic matter) and inorganic mineral related fractures (e.g., matrix mineral intergranular fractures, matrix mineral intragranular fractures, clay mineral intergranular fractures, and clay intragranular fractures). These micro-fractures are observed with the following characteristics. First, the structural micro-fractures (**Figure 9A**) are developed in mineral matrix, with flat form or serrated edges. In contrast to non-structural factures, these structural micro-fractures are generally large in size, with width of several hundreds of nanometers to microns and length of tens of microns to millimeters, even covering the whole section surface. Second, the fractures around the organic matter edge (**Figure 9B**) and fractures within the organic matter (**Figure 9C**) are micro-fractures derived from the volume variation of organic matters as a result of hydrocarbon generation and expulsion (Zhang et al., 2016b). These fractures are wide for dozens to hundreds of nanometers, with length depending on the organic matter size. Third, the shale matrix minerals include quartz, feldspar,

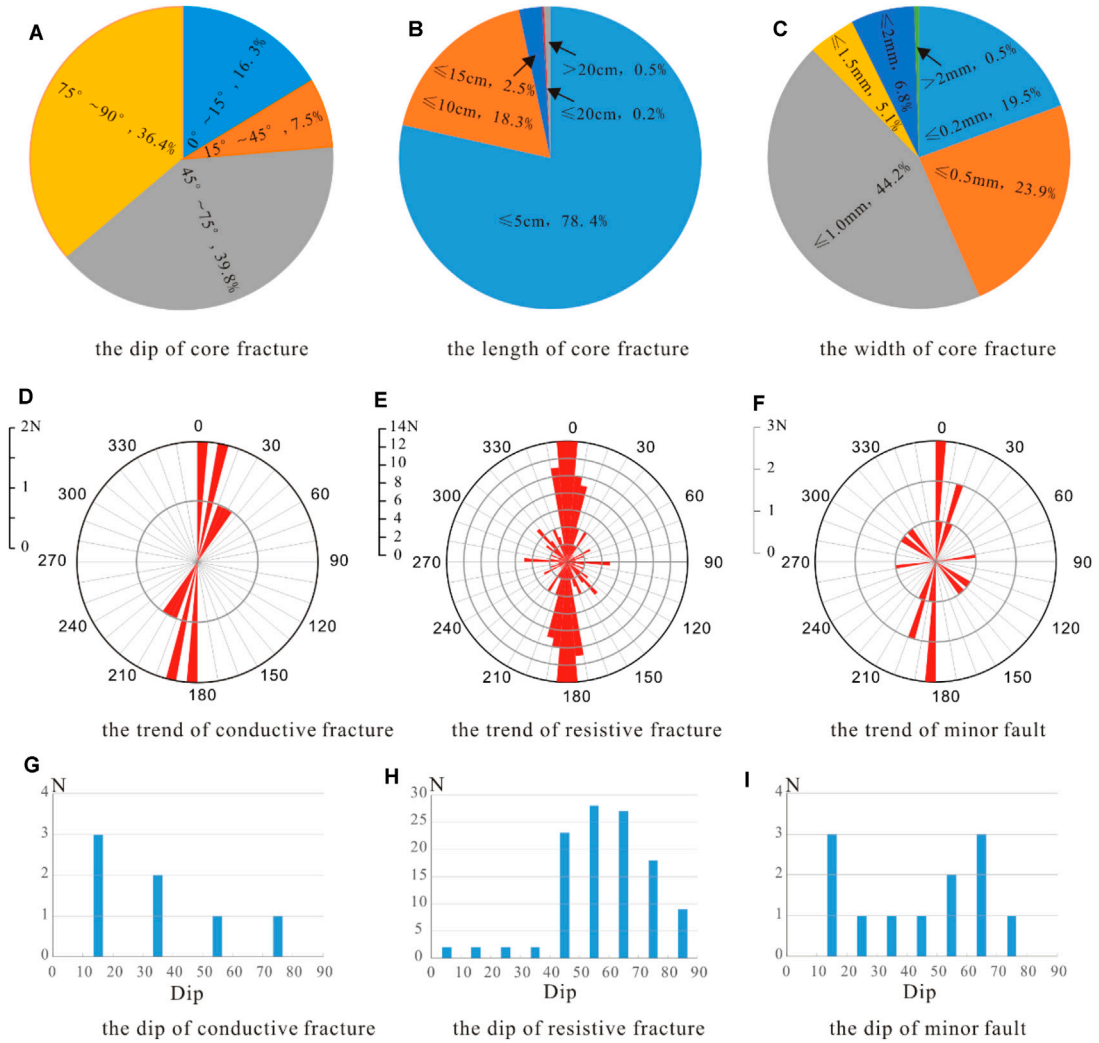

FIGURE 8 | The characteristic parameters of the fractures in cores of Niutitang shale. The structural fractures are dominated by high dip-angle and vertical fractures **(A)**; the fracture length ranges between 0 and 5 cm, followed by 5–10 cm **(B)**; the fractures with aperture ≤1.0 mm are overwhelming **(C)**; the high resistivity fractures strike in nearly NS with the dip angle of 52° **(E,H)**; the high conductivity fractures and micro-faults mainly strike in NNE-SSW **(D,F)**, with the dip angle of 58° **(G)** in dominance and between 14 and 78° **(I)**, respectively.

calcite, dolomite, pyrite and other brittle minerals. The matrix mineral intergranular/intragranular fractures were generated in such minerals at certain burial depth subject to phase transition (Wu et al., 2005), dissolution, and external force between or on crystalline grains, and due to the cleavage feature of the minerals, under certain temperature and pressure. Such fractures are generally small, with their length and width restricted by the size of crystalline grains (**Figures 9D–G**). Fourth, the clay mineral intergranular/intragranular fractures were mainly generated along with the syneresis and pressure-solution of clay minerals (Zhou et al., 2015). A large quantity of micro-fractures are observed under SEM among the silk and crinkled flake illites, with the width ranging from dozens to hundreds of nanometers or even up to 1 μm, and excellent connectivity (**Figures 9H, I**).

DISCUSSION

Dominant Factors of Fractures in Shale

This study suggests that the development of fractures in shale is mainly controlled by multiple complicated factors, either structural or non-structural, including tectonic setting, sedimentary environment, diagenetic evolution, lithological and mineral composition, organic carbon content, organic matter evolution, rock mechanics, and abnormal high pressure (Ding et al., 2012; Zhang et al., 2015; Wang et al., 2018b; Miao et al., 2020; Wang et al., 2021).

Tectonic Background

In the Upper Yangtze region, northern Guizhou Province, the marine shale experienced deep burial (highly-evolved) in the

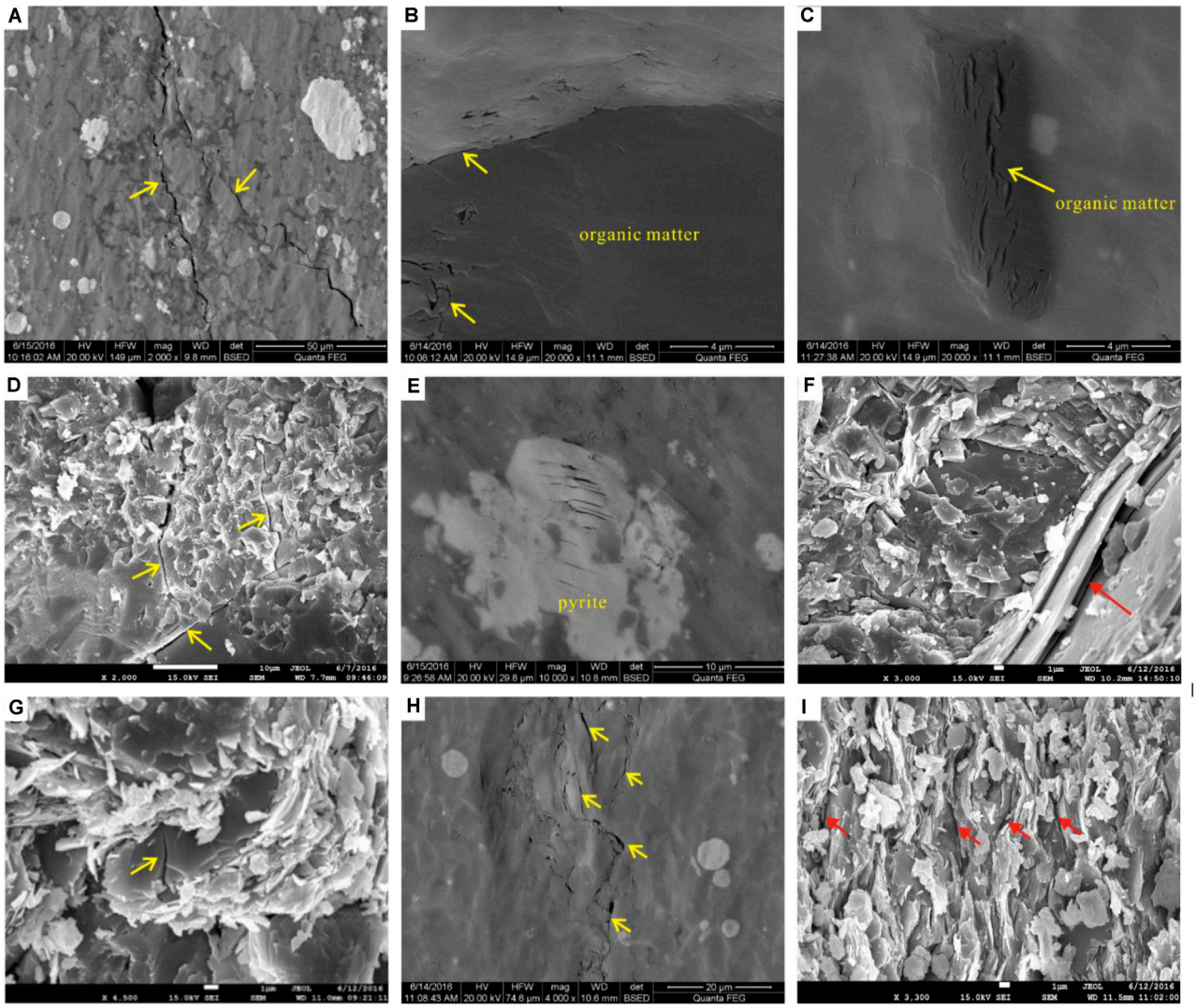

FIGURE 9 | Characteristics of the micro-fractures of the Niutitang shale. **(A)** 2014.53 m, micro-structural fractures; **(B)** 1939.94 m, fractures around the organic matter edge and fractures within the organic matter; **(C)** 1971.14 m, intra-organic matter fracture; **(D)** 1927.22 m, the intergranular micro-fracture of calcites; **(E)** 1999.31 m, the intergranular micro-fracture of pyrites; **(F)** 1985.65 m, the cleavage micro-fractures of mica; **(G)** 1939.94 m, the grain breakage fracture of feldspar; **(H)** 1963.92 m, the intergranular fractures of mud particles; **(I)** 1966.73 m, the directional arrangement of the flake clay minerals such as illite formed intergranular fractures.

early stage and strong uplifting, severe denudation and intense deformation in the late stage, along with the polycyclic evolution and multiphase tectonic superimposition and transformation (Cheng et al., 2015). This tectonic setting can be reflected by the complex characteristics and filling periods of fractures within cores from Well YX1.

Xu et al. (2017) considered that the Yanshanian period was the strongest tectonic movement during the past tectonic movements in the study area. The direction of maximum principal stress is NW-SE and the direction of minimum principal stress is NE-SW. F1 - F3 are major faults striking NNE, which were formed before the Yanshanian period and basically controlled the shape and scope of the syncline and anticline in this area; The Xieba anticlinorium, which is close to the Well YX1, was formed in the Yanshannian period. The major faults in the Xieba anticlinorium are in NE and NNE directions and the faults striking NW were also developed to a certain degree. The intersections between multistage systems are presented in this paper. The anticline has a box-shaped feature with an open core and a dip angle of only about 10°. The two wings suddenly become steep with a flexural structure. Although there is no rupture in the sharply deformed flexures, the calcite veins are extremely developed. From imaging logging data of Well YX1, the trend of high-resistivity fractures is mainly near SN, while that of high-conductivity and micro-faults mainly strike NNE-SSW. The strike of natural fractures in Well YX1 is almost consistent

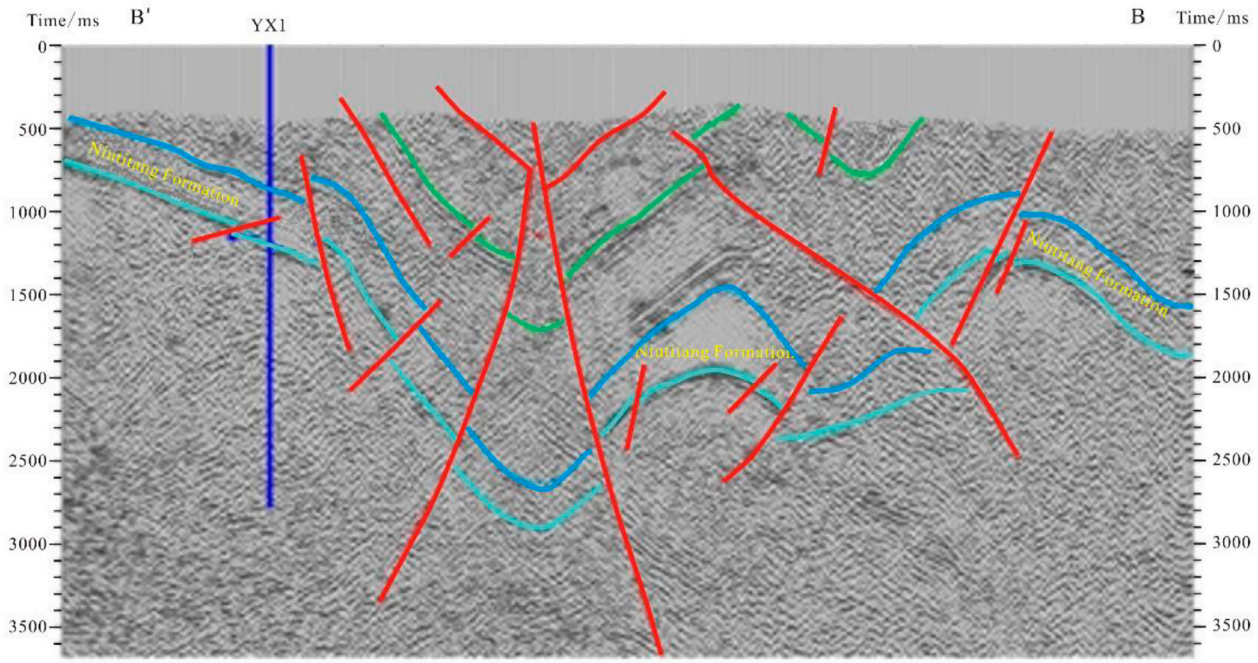

FIGURE 10 | YX1 well offset time profile. Refer to **Figure 1C** for the location of the profile.

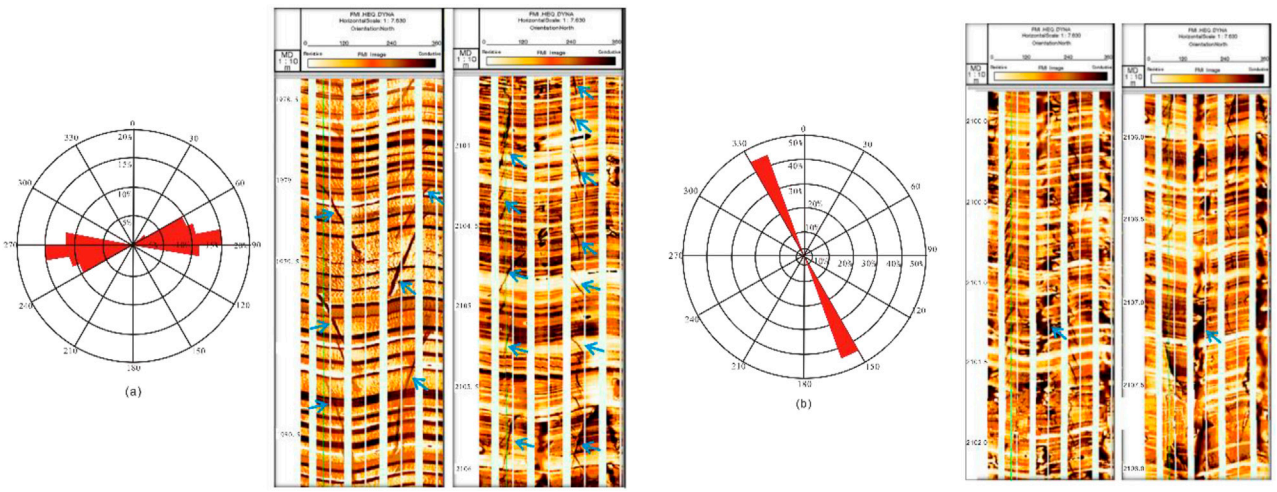

FIGURE 11 | Drilling induced fractures trend NEE-SWW **(A)** and sidewall cavings trend NNW-SSE **(B)**.

with that of F2 and faults in the Xieba anticlinorium. The fracture development is controlled by the major faults. Due to the complex geomorphological and geological conditions, the quality of 2D seismic data in this area is poor. Based on YX1 well offset time profile, and combined with well-side structure analysis based on FMI data, there might be the development of a small thrust fault crossing Well YX1 (**Figure 10**).

Affected by the current stress field, drilling induced fractures and sidewall cavings associated with current stress fields occurred during drilling (Dai et al., 2014). In the FMI image of Well YX1, the drilling induced fractures that were well developed, trending NEE-SWW (**Figure 11A**). The sidewall caving analysis indicates that the direction of the lowest horizontal principal stress near the well is NNW-SSE (**Figure 11B**). Based on the above information, the direction of present maximum horizontal principal stress in this well can be judged to be NEE-SWW, with direction of the minimum horizontal principal stress being NNW-SSE. The strike of high-conductivity fracture in Well YX1 is NNE-SSW. Willis

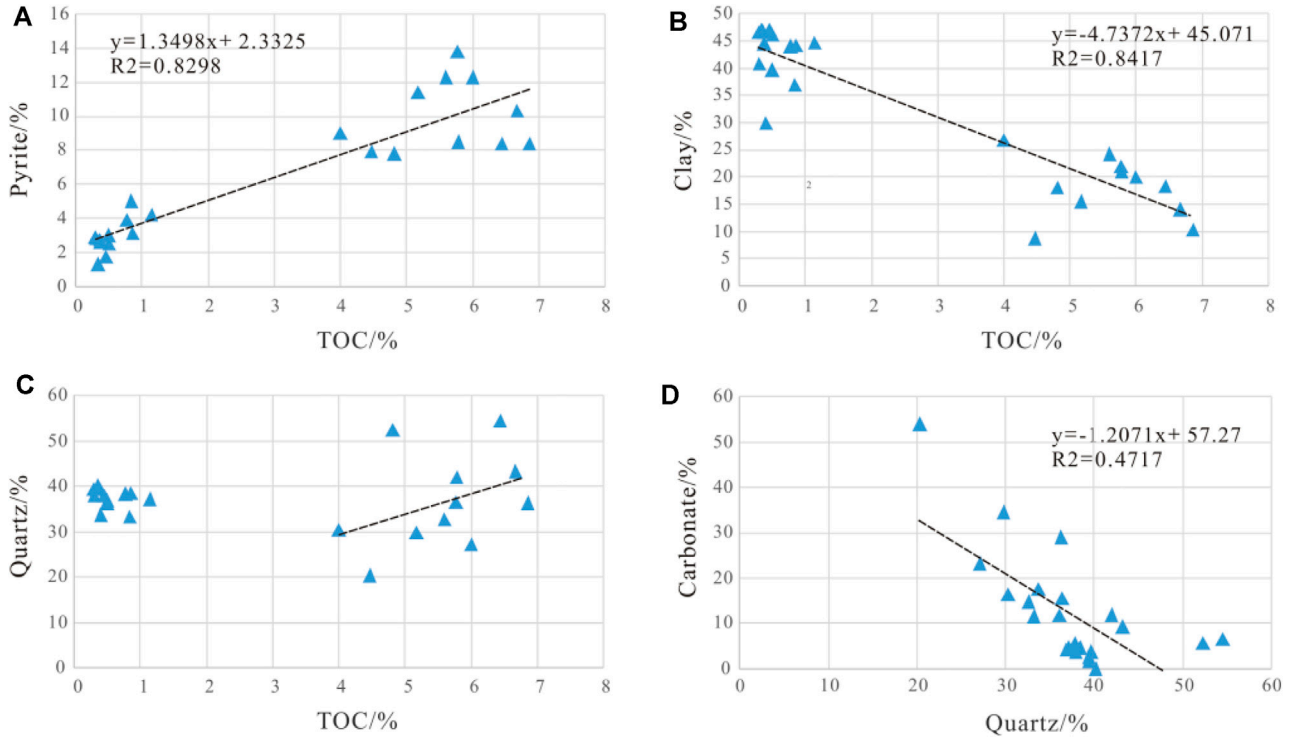

FIGURE 12 | Relationships between mineral contents and TOC of Niutitang shale. **(A)** Total content of pyrite shows a good positive correlation with TOC; **(B)** the clay mineral content is negatively related to TOC; **(C)** the quartz content for shallow continental shelf facies is stable and for deep continental shelf facies the quartz content has a positive correlation with TOC; **(D)**the contents of quartz and carbonate show an obvious negative correlation.

and Wallroth (1995) proposed that the current fracture apertures are inversely proportional to the normal stress on the fracture surface. It can be seen from above that when the direction of fractures is perpendicular to the direction of the maximum principal stress, the normal stress on the fracture surfaces is the largest and the fracture closure degree is high. When the fracture direction is perpendicular to the direction of the minimum horizontal principal stress, the normal stress on the fracture surfaces is the smallest, and the current facture apertures are large. Compared with the high-resistivity fracture mainly striking SN, the angle between the striking of the high-conductivity fracture and the present horizontal principal stress is closer to 90°, and they are easier to maintain their apertures.

Sedimentary Environment

Both lithological/mineral composition and organic carbon content imply the influences of sedimentary environment on fractures within the shale reservoir. Domestic researchers conducted an in-depth investigation on the sedimentary environment of the Lower Cambrian Niutitang Formation black shale which is widely distributed in the South China (Guo et al., 2004; Chen et al., 2006; Zhao et al., 2006; Yuan et al., 2007; Yang et al., 2009; Wu et al., 2014), and proposed that the black shale was deposited as continental shelf facies along with the anoxic event during the Qiongzhusi Age (which was synchronous to the oceanic anoxic event during the Early Tommotian Age), when the sea level rose globally and the oceanic current upwelled to bring about the prosperous bacteria and algae, which resulted in an anoxic and reducing environment. The black shale formed in such environment has high organic abundance and favorable types.

Based on observation of cores from Well YX1, pyrite generally exists between black shale layers in nodular, lenticular, disseminated, or stratified form. The framboidal pyrite, a spherical aggregation composed of microcrystals, is common under SEM, and it is a sedimentary mineral with rich organic matter, indicating a long-period anoxic sedimentary environment (Beveridge et al., 1983; Jørgensen et al., 2009). Total content of pyrite is high in fractures-developed intervals, becomes lower and stable upwards, and shows a good positive correlation with the organic carbon content (**Figures 3**, **12A**). This suggests that the strong reducing sedimentary environment is favorable for enrichment of organic matters. Wang et al. (2014) and Liang et al. (2014) believed that the seafloor hydrothermal activity occurred during the deposition of the Niutitang Formation shale, and the injection of underlying acidic hydrothermal fluids intensified the oxygen-deficiency at bottom of the Niutitang Formation, thereby improving the preservation conditions of organic matter. The existence of numerous barytocalcite, a kind of epithermal mineral, in the Niutitang Formation shale of Well YX1 is a stark example.

TABLE 2 | Summary of elastic parameters of common minerals in shale.

Minerals	E/GPa	ϒ	Reference	DEN/g•cm^{-3}	Reference	Average mass fraction/%	Average volume fraction/%
Quartz	95.94	0.07	Mavko et al. (2008)	2.65	McSkimin et al. (1965)	37.2	36.0
Clay	14.2	0.3		2.1	Castagna et al. (1985)	31.5	38.5
Plagioclase	69.02	0.35		2.62	Belikov et al. (1962)	11.3	11.1
Calcite	79.58	0.31		2.71	Peselnick and Robie (1963)	3.6	3.4
Dolomite	121	0.24		2.86	Ahrens (1995)	8.6	7.7
Pyrite	305.32	0.15		5.02		6.4	3.3

As one of the main components of black shale, quartz was supplied by a variety of sources, such as hemipelagic mud (from shallow continental shelf), and biological skeleton residue. Burial of siliceous organisms (e.g., radiolarian) resulted in high silica content in shale, which is also closely related to the organic matter content (Li et al., 2009). Qin et al. (2010) also suggested that the increase in quartz content of the black shale might be controlled biologically by plankton, benthos, and fungi. The study on correlation between TOC and quartz content (**Figure 12C**) shows that the quartz content for shallow continental shelf facies is stable and has no obvious correlation to TOC. For deep continental shelf facies the quartz content has a positive correlation with TOC. It is worth noting that the contents of quartz and carbonate (mainly dolomite) show an obvious negative correlation (**Figures 3**, **12D**). Even if the quartz content reduces, the high carbonate content can still keep the black shale in excellent brittleness, showing a tendency to generate natural fractures and artificially induced fractures.

The clay mineral content is negatively related to the organic matter abundance (**Figure 12B**), which is inconsistent with the general view that high clay mineral content must correspond to high organic matter content. Deep water and far provenance were not favorable for transportation and deposition of terrigenous clastic and clay with water in a deep continental shelf sedimentary environment (Nie and Zhang, 2012). These results indicate that, in a deep continental shelf sedimentary environment, the closer to the abyssal region, the farther the provenance, the lower the contents of clay and shale, and the higher the relative content of silicon (e.g., quartz).

Rock Mechanics and Brittleness

Rock Mechanics

Under the same stress field, the development of fractures derived from shale breakage is closely related to the rock mechanics of shale; especially, the shale with high elastic modulus and low Poisson's ratio is more brittle and likely to generate fractures (Ding et al., 2012). Based on the results of whole rock X-ray diffraction analysis, the shale elastic modulus and Poisson's ratio were calculated using the Voigt-Reuss-Hill (V-R-H) average model, which was established with the average of the Voigt (1910) upper limit and the Reuss and Angew (1929) lower limited proposed by Hill (1952). The calculation results indicate that the fracture-developed sections are characterized by high Young's modulus (E/GPa) and low Poisson's ratio (ϒ) (**Figure 3**; **Table 1**). The calculated Young's modulus and Poisson's ratio of minerals are shown in **Table 2**. Similar to other shale gas reservoirs, the Niutitang Formation shale reservoir in the study area has high elastic modulus, Poisson's ratio, and high fracturability.

Schlumberger Company conducted the logging interpretation of rock mechanics. However, abnormal changes in dynamic Young's modulus and Poisson's ratio well logs occur in the fractured interval due to many factors, for example, mass fractures reduce the mechanical strength of shale (Yu, 2013), borehole instability, and TOC content (Liu S. L. et al., 2015). The base lines, namely, the averages of Young's modulus and low Poisson's ratio for well sections with continuous and smooth logs, were overlapped (**Figure 3**), revealing that the zones with a certain area difference correspond well to the fractures-developed zones. Fracture-developed sections often broke in the process of coring; thus, the core-breaking sections of Well YX1 also well correspond to the above zones (**Figure 3**).

Brittleness

The content of brittle minerals influences the fracture development in shale. The higher the brittle mineral content, the more brittle the rock , and the more easily natural fractures are generated (Zou et al., 2010). According to the whole rock X-ray diffraction analysis, minerals in the Niutitang Formation of Well YX1 include quartz, clay, plagioclase, dolomite, pyrite, and calcite, in a descending order of content. Compared with the fracture-undeveloped sections (**Table 1**), the fracture-developed sections have much higher contents of plagioclase, dolomite, and pyrite, but remarkably lower content of clay. In general, the quartz content shows minor variation; however, in the 2011.7–2034.21 m interval, where the volume density of fractures (D_{vf}) is very large, the quartz content is 39.4% on average, up to 54.5%. Previous studies adopted different brittle minerals depending on study areas, and accordingly, in this study, the numerical simulation was used to analyze the variation of elastic modulus and Poisson's ratio with content of minerals. The average volume fraction of main minerals was estimated with the known average mass fraction (**Table 2**). The result indicates that the clay minerals, showing

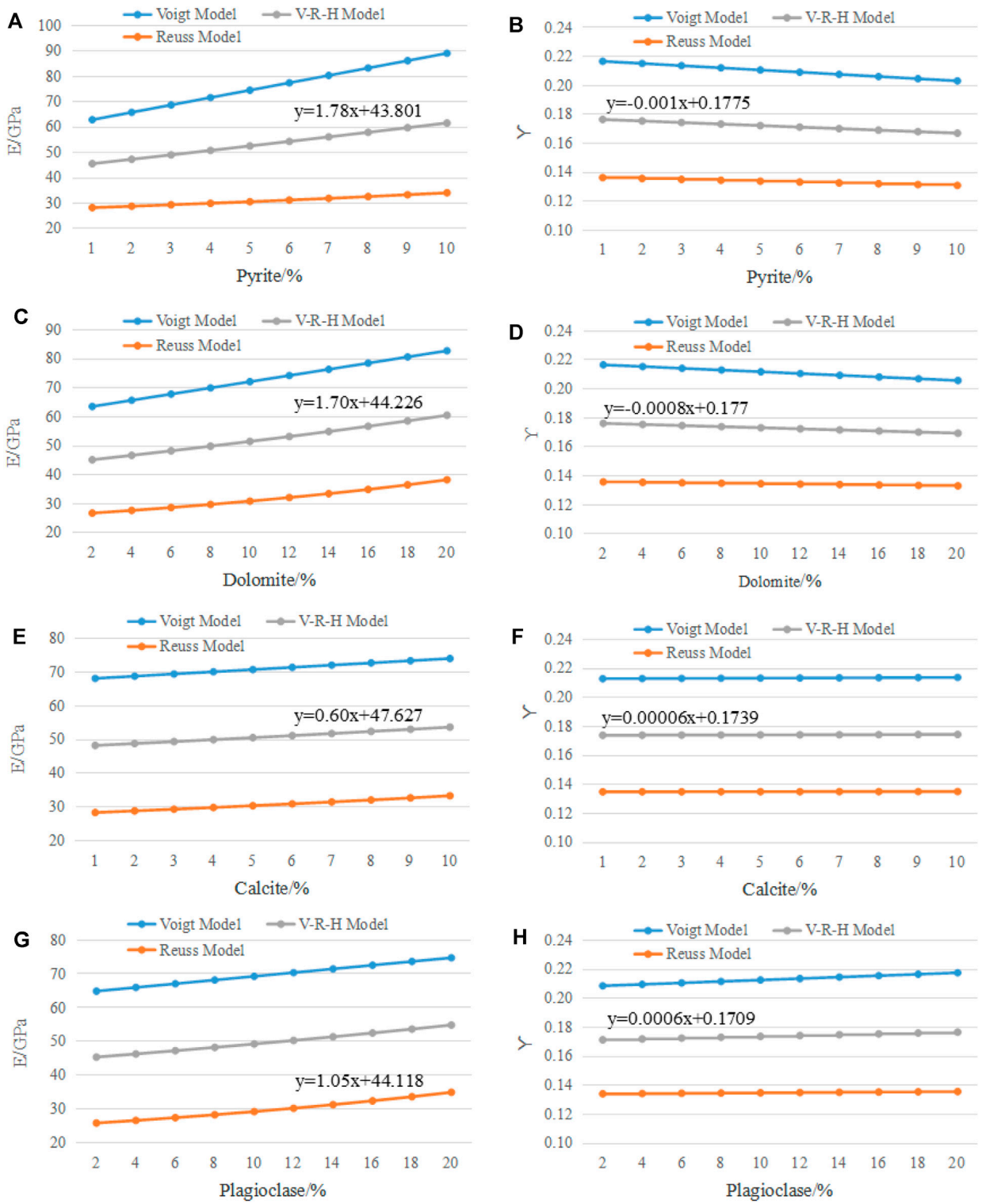

FIGURE 13 | Elastic parameters versus pyrite **(A,B)**, dolomite **(C,D)**, calcite **(E,F)** and plagioclase **(G,H)** content, respectively.

the most significant change of volume fraction with the mass fraction, have the smallest density. For Well YX1, the average volume fraction of quartz, a commonly-recognized brittle mineral, was selected and defined as a constant of 36.0%, and the V-R-H model was used to simulate the variation of elastic modulus and Poisson's ratio with the clay mineral content for plagioclase, dolomite, pyrite, and calcite. The V-R-H model simulation results show that (**Figure 13**), within the respective mineral volume fraction, the slopes of the Young's modulus fitting of pyrite, dolomite, calcite, and plagioclase is 1.78, 1.70, 0.60 and 1.05, respectively, and that of the Poisson's ratio fitting is -1×10^{-3}, -8×10^{-4},6×10^{-5} and 6×10^{-4}, respectively. The larger the slope of Young's modulus fitting, the smaller the slope of Poisson's ratio fitting, indicating that the influence of minerals on Young's modulus and Poisson's ratio is greater. Therefore, the decreasing influence of the four minerals on Young's modulus and Poisson's ratio is pyrite, dolomite, plagioclase, and calcite. It can be seen that the Young's modulus increases and the Poisson's ratio decreases as the contents of dolomite and pyrite increase, suggesting increasing brittleness. When the contents of plagioclase and calcite increase, the Young's modulus increases but the Poisson's ratio does not change greatly or tends to increase slightly (**Figure 13**). Accordingly, quartz, dolomite, and pyrite were taken as brittle minerals to calculate brittleness index in this study (BRT, **Figure 3**). It is found that the calculation results coincide with the fracture development (**Table 2**).

Different fracture presence in rocks with varied litholgies reflect macroscopically the heterogeneity of rock minerals. This study reveals the presence of fractures for siliceous shale facies, but non-presence of fractures for mixed shale facies. However, for the same lithofacies, fracture presence may be different due to the small difference in mineral composition. For mixed shale facies, fractures are more developed in the sandy mudstone with higher sand content and the fractures developed in silty mudstone are found terminating in mudstone through core analysis (**Figure 12G**). Similarly, the lithologic heterogeneity of siliceous shale facies leads to the difference in fracture development (**Figure 12H**).

TOC Content

It is generally believed that under the same mechanical background, that the organic carbon content is one of the important factors influencing the development of fractures (Wang R. Y. et al., 2015). From the top of Niutitang Formation to 1996.5 m, the TOC content is between 0.29% and 1.14%, averaging on 0.73%; from 1996.5 m to the bottom of Niutitang Formation, it ranges between 2.17% and 9.36%, with an average of 5.8%, which is obviously higher than the middle-upper sections. The organic carbon content is closely correlated with fracture development. The net-like fractures and low dip-angle slip fractures are very well-developed in the middle-lower sections with high TOC. **Figure 3** shows that the slip fractures are concentrated in the areas with high TOC—averagely 6.7%. Sayers (1995) and Hill and Nelson (2000) considered that the organic matter in shale have much weaker physico-mechanical properties than other minerals, and the organic matters result in small cohesion and internal friction angle of shale, thereby, greatly reducing the anti-shear ability, so that the shale may break to generate low dip-angle slip fractures and net-like fractures. Ding et al. (2012) made a statistical analysis on large shale gas reservoirs in China and abroad and also indicated that the higher the organic matter content, the better the fractures and micro-fractures develop.

Diagenetic Evolution and Hydrocarbon Generation

Both diagenetic evolution and hydrocarbon generation from organic matter within shale might produce abnormal fluid pressure (Kobchenko et al., 2011; Nguyen et al., 2013), which has apparent influences on the development of micro-fractures. Rock often breaks to generate micro-fractures when the pore fluid pressure exceeds the minimum principal stress and the tensile strength of the rock (Jones, 1981). The abnormal pressure in strata may counteract the confining pressure to a certain extent, so that the effective stress acting on the rock diminishes and the Mohr's stress circle moves leftward as a whole to approach the rock rupture envelope, making the rock more prone to breakage. When the abnormal fluid pressure reaches a certain value, the minimum principal stress changes from positive (compressive stress) to negative (tensile stress), forming extensional fractures perpendicular to the minimum principal stress (Zeng and Li, 2010).

The evolution and combination of clay minerals can reflect the diagenetic stage and maturity. The clay minerals in the Niutitang Formation of Well YX1 contain abundant illite (average mass fraction of 78.5%), I/S layer and chlorite, without kaolinite, illustrating Phase B of late diagenetic stage, which corresponds to the evolution stage of high maturity and over-maturity. Micro-fractures in the clay minerals exist mainly among grains of illite. Hydrocarbon generation from organic matter induced fractures around the organic matter edge and fractures within the organic matter. However, with the further increase of organic matter maturity, pores, and fractures associated with organic matter decrease in size. Zhao et al. (2018) proved in their study on the characteristics of Niutitang Formation shale in western Hunan-Hubei region that high evolution could lead to the carbonization of shale with high abundance, thus diminishing the quantity of organic pores and fractures. Yang et al. (2016) discovered a positive correlation between the desorbed gas volume and the micro-fracture volume ratio when they investigated the relationship between micro-fracture development and gas content. Highly-evolved organic pores and fractures are not developed well in the Niutitang Formation shale of Well YX, which is not favorable for the shale gas adsorption and accumulation.

In conclusion, based on the above analysis, tectonic background, rock mechanics, brittleness, and TOC content are the main factors of structural fractures, the bedding fractures in non-structural fractures are mainly controlled by sedimentary environment, while the overpressure fractures are mainly affected by diagenetic evolution and hydrocarbon generation.

Control of Faults and Fractures on Shale Gas

The shale in Well YX1 is characterized by large thickness (nearly 40 m), high abundance of organic matter (average TOC of 5.8%), high–over maturity, presence of matrix pores (average porosity of 3.2%), and part of the fractures have a certain aperture, presenting favorable evidence for "geological sweet spots". Moreover, it is dominated by siliceous shale facies, with comparable elastic modulus, Poisson's ratio, and brittleness to other global shale gas reservoirs (Abousleiman et al., 2007; Sone and Zoback, 2010; Koesoemadinata et al., 2011; Kumar et al., 2012; Li et al., 2012; Wang R. Y. et al., 2016b), recording as good conditions for "engineering sweet spots". Therefore, the key factors for why the shale gas of Well YX1 cannot form industrial gas flow may be attributed to fault and fracture damage to the reservoir. According to the available shale gas accumulation mechanism, the primary shale gas reservoir should be in abnormal high pressure (Zhang et al., 2004). However, according to the pore pressure logging results (**Figure 3**), the pore pressure of the Niutitang Formation in the well ascends gently from top to bottom, without occurrence of overpressure. The Barnett, Marcellus, and Haynesville shale plays in the US are characterized by obvious overpressure (Li et al., 2007; Liang and Yu, 2016). After years of exploration, people gradually realized that due to the complex tectonic background of marine shale in southern China, it is necessary to consider formation pressure as a key parameter for shale gas reservoirs (Liang and Yu, 2016; Liu et al., 2021).

Based on the formation dip-angle data, the occurrence of organic-rich shale reservoir in this well is similar to the underlying and overlying strata, but varies greatly within reservoir itself (**Figure 3**). Compared with the upper and lower strata, the strata of a 2010–2030 m interval tends to deflect clockwise by approximately 90°, indicating that there is obvious deformation in this interval. Moreover, a lot of natural fractures are found in the cores taken from this interval, and most of them cut rock layers in net-like manner, as proved by core breaking and crumpling. In summary, the phenomena of variance in stratigraphic occurrences and development of a large number of fractures all indicate that faults or folds may be developed near 2010–2030 m. The two-dimensional geological data and well-side structure analysis also confirm this view (**Figure 10**). Faults or folds communicate with other formations, resulting in the escape of shale gas and damaging the overpressure environment. Therefore, it is very favorable for shale gas reservoirs to form small-scale fractures due to tectonic movements without large faults or fractures.

CONCLUSION

(1) Macro fractures are common in the Niutitang Formation, which can be divided into structural fractures and non-structural fractures. The structural fractures, being dominant, can be divided into shear fractures (e.g., high dip-angle shear fractures and low dip-angle slip fractures), extensional fractures, and tensional-shear fractures. The non-structural fractures are represented by bedding fractures and overpressure fractures. Macro-fractures are mostly filled with diverse fillings which represent varied morphologies and contact relationships under microscope. The fillings include calcite, quartz, dolomite, and pyrite, as well as anhydrite occasionally. The staggered relationships of fractures prove the complexity of tectonic movements in the study area. The Niutitang Formation shale reservoir of Well YX1 has micro-fractures with the dominance of non-structural fractures, which can be divided into organic matter related fractures (e.g., fractures around the organic matter edge and fractures within the organic matter) and inorganic mineral related fractures (e.g., matrix mineral intergranular fractures, matrix mineral intragranular fractures, clay mineral intergranular fractures, and clay intragranular fractures).

(2) The formation of structural fractures in Well YX1 is mainly controlled by the major fault. The influence of mineral composition and content, mechanical properties, brittleness, and organic matter content of rocks on the fracture development are the external manifestation of the sedimentary environment. The organic matter related fractures are not common due to diagenetic evolution. The Lower Cambrian Niutitang Formation organic-rich shale of Well YX1 is characterized by organic matters in favorable type and high abundance, rich silicon, high pyrite content, and high dolomite content in intervals with low silicon content. It was deposited as continental shelf facies along with the anoxic event during the Qiongzhusian Age (which was synchronous to the oceanic anoxic event during the Early Tommotian Age). The simulation using V-R-H model shows that, in addition to quartz, a commonly-recognized brittle mineral, the increase in dolomite and pyrite contents leads to increase in the elastic modulus and decrease in the Poisson's ratio, thus increasing the rock brittleness. Therefore, this type of organic-rich shale not only easily forms fractures, but is also conducive to fracturing.

(3) Compared with the shale gas reservoirs at home and abroad, the organic-rich shale reservoirs in Well YX1 have both conditions of "geological sweet spots" and "engineering sweet spots". However, strong tectonic movements have formed inter-strata faults that lead to the loss of shale gas and damage to the overpressure environment. Therefore, for fractures, small-scale fractures due to tectonic movement without large inter-strata faults are most favorable to shale gas reservoirs. Based on the complex tectonic setting in northern Guizhou Province, it is necessary to strengthen this work by finding a better confined area of pressure in the region.

DATA AVAILABILITY STATEMENT

The original contributions presented in the study are included in the article/Supplementary Material, further inquiries can be directed to the corresponding authors.

AUTHOR CONTRIBUTIONS

XZ: Conceptualization, Methodology, Formal analysis, Resources, Writing-original draft, Writing-review and editing; RW: Methodology, Investigation, Supervision, Editing and revision ZD: Conceptualization, Methodology, Supervision, Funding acquisition; JW: Methodology, Funding acquisition; ZW: Conceptualization, Methodology; WD: Editing and revision; AL: Resources, Writing-original draft; ZX: Writing-review and editing; ZC: Methodology, Investigation; XW: Formal analysis, Resources; All authors reviewed the article.

FUNDING

This research was supported by the National Natural Science Foundation of China (No. 41902134 and 42172165) and SINOPEC Ministry of Science and Technology Project (No. P20046-1).

ACKNOWLEDGMENTS

We would like to thank the staff at the laboratories that helped in performing the tests and analyses. We are also grateful to the editors and reviewers for their revisions and comments.

REFERENCES

Abousleiman, Y., Tran, M., and Hoang, S. (2007). "Geomechanics Field and Laboratory Characterization of Woodford Shale: The next gas play," in *Society of Petroleum Engineers*, Anaheim, California, USA.

Ahrens, T. J. (1995). *A Handbook of Physical Constants*. Chicago: American Geophysical Union.

Anders, M. H., Laubach, S. E., and Scholz, C. H. (2014). Microfractures: a Review. *J. Struct. Geology.* 69, 377–394. doi:10.1016/j.jsg.2014.05.011

Belikov, B. P. (1962). Elastic Properties of Rocks. *Stud. Geophys. Geod.* 6, 75–85. doi:10.1007/BF02590043

Beveridge, T. J., Meloche, J. D., Fyfe, W. S., and Murray, R. G. E. (1983). Diagenesis of Metals Chemically Complexed to Bacteria: Laboratory Formation of Metal Phosphates, Sulfides, and Organic Condensates in Artificial Sediments. *Appl. Environ. Microbiol.* 45 (3), 1094–1108. doi:10.1128/aem.45.3.1094-1108.1983

Bisdom, K., Bertotti, G., and Bezerra, F. H. (2017). Inter-well Scale Natural Fracture Geometry and Permeability Variations in Low-Deformation Carbonate Rocks. *J. Struct. Geology.* 97, 23–36. doi:10.1016/j.jsg.2017.02.011

Bour, O., and Lerche, I. (1994). Numerical Modelling of Abnormal Fluid Pressures in the Navarin Basin, Bering Sea. *Mar. Pet. Geology.* 11 (4), 491–500. doi:10.1016/0264-8172(94)90082-5

Castagna, J. P., Batzle, B. L., and Eastwood, R. L. (1985). Relationships Between Compressional Wave and Shear Wave Velocities in Clastic Silicate Rocks. *Geophysics* 50 (4), 571–581. doi:10.1190/1.1441933

Chen, L., Zhong, H., Hu, R. Z., and Xiao, J. F. (2006). Composition of Organic Carbon Isotope of Early Cambrian Black Shale in the Xiang-qian Area and its Significances. *Jmineral Petrol.* 26 (1), 81–85. doi:10.3969/j.issn.1000-0569.2006.09.018

Cheng, L. Y., Yong, Z. Q., Wang, T. Y., Lan, N., Yu, J. Y., and Deng, B. (2015). Evaluation index of Shale Gas Preservation for Niutitang Formation in the strong Transformation Zone. *Nat. Gas Geosci.* 26 (12), 2408–2416.

Cho, Y., Ozkan, E., and Apaydin, O. G. (2013). Pressure-dependent Natural-Fracture Permeability in Shale and its Effect on Shale-Gas Well Production. *SPE Reserv.Eval. Eng.* 16 (2), 216–228. doi:10.2118/159801-pa

Clarkson, C. R., Haghshenas, B., Ghanizadeh, A., Qanbari, F., Williams-Kovacs, J. D., Riazi, N., et al. (2016). Nanopores to Megafractures: Current Challenges and Methods for Shale Gas Reservoir and Hydraulic Fracture Characterization. *J. Nat. Gas Sci. Eng.* 31, 612–657. doi:10.1016/j.jngse.2016.01.041

Dai, J. S., Shang, L., Wang, T. D., and Jia, K. F. (2014). Numerical Simulation of Current in-situ Stress Field of Fengshan Formation and Distribution Prediction of Effective Fracture in Futai Buried Hill. *PGRE* 21 (6), 33–36. doi:10.13673/j.cnki.cn37-1359/te.2014.06.008

Diao, H. Y. (2013). Rock Mechanical Properties and Brittleness Evaluation of Shale Reservoir. *Acta Petrologica Sinica* 29 (9), 3300–3306.

Ding, W. L., Li, C., Li, C. Y., Jiu, K., and Zeng, W. T. (2012). Dominant Factor of Fracture Development in Shale and its Relationship to Gas Accumulation. *Earth Sci. Front.* 19 (2), 212–220. (In Chinese).

Ding, W. L. (2015). *Study of Fracture Identification Methods and Characteristics on Unconventional Oil and Gas Reservoirs*. Beijing: Geological Publishing House, 72–73.

Du, J. F., Yang, H., and Xu, C. C. (2011). A Discussion on Shale Gas Exploration and Development in China. *Nat. Gas Industry* 31 (5), 6–8. doi:10.3787/j.issn.1000-0976.2011.05.002

Durney, D. W., and Ramsay, J. G. (1973). "Incremental Strains Measured by Syntectonic crystal Growths," in *Gravity and Tectonics*. Editors KA De Jong and K Scholten (New York: Wiley), 67–96.

Gale, J. F. W., Laubach, S. E., Olson, J. E., Eichhuble, P., and Fall, A. (2014). Natural Fractures in Shale: A Review and New Observations. *Bulletin* 98 (11), 2165–2216. doi:10.1306/08121413151

Gomez, L. A., and Laubach, S. E. (2006). Rapid Digital Quantification of Microfracture Populations. *J. Struct. Geology.* 28 (3), 408–420. doi:10.1016/j.jsg.2005.12.006

Gu, Y., Xu, S., Zhang, W., Xu, J. J., and Zhai, Z. Y. (2021). Fracture Development Characteristics and Geological Significance of Longmaxi Formation Shale in Northern Guizhou. *Fault-Block Oil & Gas Field* 28 (06), 733–738. doi:10.6056/dkyqt202106003

Guo, Q,J., Liu, C. Q., Strauss, H., and Goldberg, T. (2004). Isotopic Investigation of Late Neoproterozoic and Early Cambrian Carbon Cycle on the Northern Yangtze Platform, south china. *Acta Geoscientica Sinica* 25 (2), 151–156.

Guo, X. S., Li, Y. P., Liu, R. B., and Wang, Q. B. (2014). Characteristics and Controlling Factors of Micro-pore Structures of Longmaxi Shale Play in the Jiaoshiba Area, Sichuan Basin. *Nat. Gas Industry* 34 (6), 9–16. doi:10.3787/j.issn.1000-0976.2014.06.002

Han, G., He, F., and Zhang, X. Z. (2019). Application of Array Acoustic Logging to Fracture Identification:A Case Study of Area K in Ordos Basin. *Pet. Geology. Recovery Efficiency* 26 (03), 63–69. doi:10.13673/j.cnki.cn37-1359/te.2019.03.008

He, Z. L., Nie, H. K., and Zhang, Y. Y. (2016). The Main Factors of Shale Gas Enrichment of Ordovician Wufeng Formation-SilurianLongmaxi Formation in the Sichuan Basin and its Adjacent Areas. *Earth Sci. Front.* 23 (2), 8–017.

Hill, D. G., and Nelson, C. R. (2000). Gas Productive Fractured Shales: An Overview and Update. *Gas Tips Gas Res. Inst.* 6 (2), 4–13.

Hill, R. (1952). The Elastic Behaviour of a Crystalline Aggregate. *Proc. Phys. Soc. A.* 65 (5), 349–354. doi:10.1088/0370-1298/65/5/307

Hou, G. T., and Pan, W. Q. (2013). *Fracture Geological Modeling and its Mechanism*. Beijing: SciencePress.

Hu, D. F., Zhang, H. R., Ni, K., and Yu, G. C. (2014). Main Controlling Factors for Gas Preservation Conditions of marine Shales in southeastern Margins of the Sichuan Basin. *Nat. Gas Industry* 34 (6), 17–23. doi:10.3787/j.issn.1000-0976.2014.06.003

Jiu, K. (2014). *Reservoir Characterization and Evation of Paleozoic Shale in Fenggang Guizhou and Surrounding Areas*. PhD thesis. Beijing (Haidian), China: China University of Geosciences, 13–18. doi:10.27493/d.cnki.gzdzy.2014.000016

Jones, R. W. (1981). Some Mass Balance and Geological Constraints on (Oil) Migration Mechanisms. *Am. Assoc. Pet. Geol. Bull. (United States* 65 (1), 103–122. doi:10.1306/2f91977e-16ce-11d7-8645000102c1865d

Jørgensen, C. J., Jacobsen, O. S., Elberling, B., and Aamand, J. (2009). Microbial Oxidation of Pyrite Coupled to Nitrate Reduction in Anoxic Groundwater Sediment. *Environ. Sci. Technol.* 43 (13), 4851–4857. doi:10.1021/es803417s

Kassis, S., and Sondergeld, C. H. (2010). Fracture Permeability of Gas Shale: Effects Ofroughness, Fracture Offset, Proppant, and Effective Stress. *Soc. Pet. Eng, J.* 131376, 1–17. doi:10.2118/131376-ms

Kobchenko, M., Panahi, H., Renard, F., Dysthe, D. K., Malthe-Sørenssen, A., Mazzini, A., et al. (2011). 4D Imaging of Fracturing in Organic-Rich Shales during Heating. *J. Geophys. Res.* 116, B12201. doi:10.1029/2011jb008565

Kosari, E., Ghareh-Cheloo, S., Kadkhodaie-Ilkhchi, A., and Bahroudi, A. (2015). Fracture Characterization by Fusion of Geophysical and Geomechanical Data: a Case Study from the Asmari Reservoir, the central Zagros Fold-Thrust belt. *J. Geophys. Eng.* 12 (1), 130–143. doi:10.1088/1742-2132/12/1/130

Koesoemadinata, A., El-Kaseeh, G., and Banik, N. (2011). "Seismic Reservoir Characterization in Marcellus Shale," in *Society of Petroleum Engineers*, San Antonio, Texas.

Kumar, V., Sondergeld, C. H., and Rai, C.S. (2012). "Nano to Macro Mechanical Characterization of Shale," in *Society of Petroleum Engineers*, San Antonio, Texas, USA.

Lang, X. L., Guo, Z. J., and Liu, H. Q. (2014). Combination of Well Logging with Seismic Data in theIdentification and Prediction of Fractures and Cave. *J. Southwest Pet. University(Science Techn. Edition)* 36 (04), 12–20. doi:10.11885/j.issn.1674-5086.2012.11.27.01

Laubach, S. E. (2003). Practical Approaches to Identifying Sealed and Open Fractures. *Bulletin* 87 (4), 561–579. doi:10.1306/11060201106

Li, G., Liu, H., and Meng, Y. (2012). "Challenges in Deep Shale Gas Drilling: A Case Study in Sichuan Basin," in *Society of Petroleum Engineers*, Tianjin, China.

Li, S. J., Yuan, Y. S., Sun, W., Sun, D. S., and Jin, Z. J. (2016). The Formation and Destroyment Mecha-Nism of Shale Gas Overpressure and its Main Controlling Factors in Silurian of Sichuan Basin. *Nat. Gas Geosci.* 27 (5), 924–931. doi:10.11764/j.issn.1672-1926.2016.05.0924

Li, X. J., Lu, Z. G., and Dong, D. Z. (2009). Geologic Controls on Accumulation of Shale Gas in North America. *Nat. Gas Industry* 29 (5), 27–32. doi:10.3787/j.issn.1000-0976.2009.05.006

Li, X. J, Hu, S. Y., and Cheng, K. M. (2007). Suggestions From the Development of Fractured Shale Gas in North America. *Pet. Explor. Dev.* 34 (4), 392–400. doi:10.3321/j.issn:1000-0747.2007.04.002

Li, Z. W., Pan, R. F., Shao, Y., and Yang, B. G. (2015). Comparative Study on Reservoir Spaces and Occurrence Ways of Shale Gas and Oil. *J. Chongqing Univ. Sci. Techn. (Natural Sci. Edition)* 17 (5), 1–4. doi:10.3969/j.issn.1673-1980.2015.05.001

Liang, Y., Hou, D. J., Zhang, J. C., and Yang, Q. G. (2014). Hydrothermal Activities on the Seafloor and Evidence of Organic-Rich Sourcerock from the Lower Cambrian Niutitang Formation, Northwestern Guizhou. *Pet. Geology. Recovery Efficiency* 21 (4), 28–32. doi:10.13673/j.cnki.cn37-1359/te.2014.04.007

Liang, Z. Z., and Yu, T. H. (2016). Research Status and Exploration Enlightenment on Over-pressure and Enrichment Shale Gas in North America. *Coal Sci. Techn.* 44 (10), 161–166. doi:10.13199/j.cnki.cst.2016.10.030

Liu, D. D., Guo, J., Pan, Z. K., Du, W., Zhao, F. P., Chen, W., et al. (2021). Overpressure Evolution Process in Shale Gas Reservoir: Evidence from the Fluid Inclusions in the Fractures of Wufeng Formation-Longmaxi Formation in the Southern Sichuan Basin. *Nat. Gas Industy* 41 (09), 12–22. doi:10.3787/j.issn.1000-0976.2021.09.002

Liu, J. Z., Sun, Q. Y., Xu, G. M., and Chen, F. (2008). *Study on reservoir fractures in oil and gas fields*. Beijing: petroleum industry press.

Liu, S. L., Li, H., and Zhang, Y. C. (2015). Analysis of TOC Content Influence on Shale Brittleness Index Evaluation. *Well Logging Thchnology* 39 (3), 352–356. doi:10.16489/j.issn.1004-1338.2015.03.018

Liu, Y. X., Yu, L. J., Zhang, Q. Z., Bao, F., and Lu, Y. F. (2015). Mineral Composition and Microscopic Reservoir Features of Longmaxi Shales in southeastern Sichuan Basin. *Pet. Geology. Exp.* 37 (3), 328–333. doi:10.11781/sysydz201503328

Long, P. Y., Zhang, J. C., Tang, X., Nie, H. K., Liu, Z. J., Han, S. B., et al. (2011). Feature of Muddy Shale Fissure and its Effect F or Shale Gas Exploration and Development. *Nat. Gas Geosci.* 22 (3), 525–532.

Ma, C. F., Dong, C. M., Luan, G. Q., Lin, C. Y., Liu, X. Q., and Derek, E. (2016). Types, Characteristics and Effects of Natural Fluid Pressure Fractures in Shale: A Case Study of the Paleogene Strata in Eastern China. *Pet. Exploration Develop.* 43 (4), 580–589. doi:10.1016/s1876-3804(16)30074-x

Mavko, G., Mukerji, T., and Dworkin, J. (2008). *The Rock physics hand-book: tools for seismic analysis in porous media*. Translated by H. B. Xu and J. C. Dai (Hefei: Press of University of Scienceand Technology of China), 260–263.

McSkimin, H. J., Andreatch, P., and Thurston, R. N. (1965). Elastic Moduli of Quartz vs. Hydrostatic Pressure at 25°C and 195.8°C. *J. Appl. Phys.* 36, 1624–1632. doi:10.1063/1.1703099

Miao, F. B., Peng, Z. Q., Wang, Z. X., Yu, Y. N., Ma, Y., and Shui, Z. H. (2020). Development Characteristics and Major Controlling Factors of Shale Fractures in the Lower Cambrian Miutitang Formation, Western Margin of Xuefeng Uplift. *Bull. Geol. Sci. Techn.* 39 (02), 31–42. doi:10.19509/j.cnki.dzkq.2020.0204

Moumni, Y., Msaddek, M. H., Chermiti, A., Chenini, I., Mercier, E., and Dlala, M. (2016). Quantitative Analysis of Fractured Carbonate Reservoir and Hydrodynamic Implications: Case Study of Horchane-Braga basin (central tunisia). *J. Afr. Earth Sci.* 124, 311–322. doi:10.1016/j.jafrearsci.2016.09.016

M. Pagel, V. Barbin, P. Blanc, and D. Ohnenstetter (Editors) (2000). *Cathodoluminescence in Geosciences* (New York: Springer-Verlag).

Nelson, R. A. (1985). *Geologic Analysis of Naturally Fractured Reservoirs*. Houston, TX: Gulf PublishingCompany.

Nguyen, B. T. T., Jones, S. J., Goulty, N. R., Middleton, A. J., Grant, N., Ferguson, A., et al. (2013). The Role of Fluid Pressure and Diagenetic Cements for Porosity Preservation in Triassic Fluvial Reservoirs of the central Graben, north Sea. *Bulletin* 97 (8), 1273–1302. doi:10.1306/01151311163

Nie, H. K., and Zhang, J. C. (2012). Shale Gas Accumulation Conditionsand Gas Content Calculation: A Case Study of Sichuan Basin and Itsperiphery in the Lower Paleozoic. *Acta Geologica Sinica* 86 (2), 349–361.

Pecharsky, V. K., and Zavalij, P. Y. (2003). *Fundamentals of Powder Diffraction and Struc-Tural Characterization of Minerals*. New York: Kluwer Academic Publishers, 713.

Peselnick, L., and Robie, R. A. (1963). Elastic Constants of Calcite. *J. Appl. Phys.* 34, 2494–2495. doi:10.1063/1.1702777

Pu, B. L., Dong, D. Z., Wu, S. T., Er, C ., Huang, J. L., and Wang, Y. M. (2014). Microscopic Space Types of Lower Paleozoic marine Shale in Southern Sichuan Basin. *J. China Univ. Pet. (Edition Nat. Sci.)* 38 (4), 19–25. doi:10.3969/j.issn.1673-5005.2014.04.003

Qin, J. Z., Shen, B. J., Fu, X. D., Tao, G. L., and Teng, G. E. (2010). Ultram Icroscopic Organic Petrology and Potential of Hydrocarbon Generation and Expulsion of Quality marine Source Rocks in South China. *Oil&gas Geology.* 31 (6), 826–837. doi:10.1016/S1876-3804(11)60008-6

Ramsay, J. G. (1980). The Crack-Seal Mechanism of Rock Deformation. *Nature* 284, 135–139. doi:10.1038/284135a0

Reuss, A., and Angew, Z. (1929). Berechnung der Fließgrenze von Mischkristallen auf Grund der Plastizitätsbedingung für Einkristalle. *Z. Angew. Math. Mech.* 9 (1), 49–58. doi:10.1002/zamm.19290090104

Sayers, C. M. (1995). Simplified Anisotropy Parameters for Transversely Isotropic Sedimentary Rocks. *Geophysics* 60, 1933–1935. doi:10.1190/1.1443925

Sipple, R. F. (1968). Sandstone Petrology, Evidence from Luminescence Petrography. *J. Sediment. Petrol.* 38, 530–554.

Slatt, R. M., and Abousleiman, Y. (2011). Merging Sequence Stratigraphy and Geomechanics for Unconventional Gas Shales. *The Leading Edge* 30 (3), 274–282. doi:10.1190/1.3567258

Sone, H., and Zoback, M. D. (2010). "Strength, Creep and Frictional Properties of Gas Shale Reservoir Rocks" in *Society of Petroleum Engineers* Salt Lake City, UT.

Voigt, W. (1910). *Lehrbuch der Kristallphysik*. Leipzig: Tuebner.

Wang, J. L., Zhu, Y. M., Gong, Y. P., and Fang, H. H. (2015). Influential Factors and Forecast of Microcrack Development Degree of Longmaxi Formation Shales in Nanchuan Region, Chongqing. *Nat. Gas Geosci.* 26 (8), 1579–1586. doi:10.11764/j.issn.1672-1926.2015.08.1579

Wang, M., Chen, Y., Xu, X. Y., Zhang, X. J., Han, Y., Wang, C. J., et al. (2015). Progress on Formation Mechanism of the Fibrous Veins in Mudstone and its Implications to Hydrocarbon Migration. *Adv. Earth Sci.* 30 (10), 1 107. doi:10.11867/j.issn.1001-8166.2015.10.1107

Wang, R. Y., Ding, W. L., Gong, D. J., Leng, J. G., Wang, X. H., and Yin, S. (2015). Logging Evaluation Method and its Application for Total Organic Carbon Content in Shale: A Case Study on the Lower Cambrian Niutitang Formation in Cengong Block, Guizhou Province. *J. China Coal Soc.* 40 (12), 2874–2883.

Wang, R. Y., Ding, W. L., Gong, D. J., Leng, J. G., Wang, X. H., Yin, S., et al. (2016). Gas Preservation Conditions of marine Shale in Northern Guizhou Area: A Case Study of the Lower Cambrian Niutitang Formation in the Cen'gong Block, Guizhou Province. *Oil Gas Geology*. 37 (01), 45–55. doi:10.11743/ogg20160107

Wang, R. Y., Ding, W. L., Gong, D. J., Zeng, W. T., Wang, X. H., Zhou, X. H., et al. (2016b). Development Characteristics and Major Controlling Factors of Shale Fractures in the Lower Cambrian Niutitang Formation, southeastern Chongqing-Northern Guizhou Area. *Acta Petrolei Sinica* 37 (7), 832–845. doi:10.7623/syxb201607002

Wang, R. Y., Wang, X. H., Gong, D. J., Yin, S., Fu, F. Q., and Chen, E. (2018a). Development Features and Dominant Controlling Factors of Fractors in the Lower Cambrian Shale in South-Eastern Guizhou Area. *J. Northeast Pet. Univ.* 42 (03), 56–64. doi:10.3969/j.issn.2095-4107.2018.03.006

Wang, R. Y., Hu, Z. Q., Liu, J. S., Wang, X. H., Gong, D. J., and Yang, T. (2018b). Comparative Analysis of Characteristics and Controlling Factors of Fractures in marine and continental Shales: A Case Study of the Lower Cambrian in Cengong Area, Northern Guizhou Province. *Oil Gas Geology*. 39 (04), 631–640. doi:10.11743/ogg20180401

Wang, R. Y., Hu, Z. Q., Zhou, T., Bao, H. Y., Wu, J., Du, W., et al. (2021). Characteristics of Fractures and Their Significance for Reservoirs in Wufeng-Longmaxi Shale, Sichuan Basin and its Periphery. *Oil Gas Geology*. 42 (06), 1295–1306. doi:10.11743/ogg20210605

Wang, Y. F., Leng, J. G., Li, P., and Li, F. (2016). Characteristics and its Main Enrichment Controlling Factorsof Shale Gas of the Lower Cambrian Niutitang Formationin Northeastern Guizhou Province. *J. Palaeogeogr.* 18 (4), 605–614. doi:10.7605/gdlxb.2016.04.045

Wang, Y., Jin, C., Wang, L. H., Wang, J. Q., Jiang, Z., Wang, Y. F., et al. (2015b). Characterization of Pore Structures of Jiulaodong Formation Shale in the Sichuan Basin by SEM with Ar-Ion Milling. *Rock Mineral. Anal.* 34 (3), 278–285. doi:10.15898/j.cnki.11-2131/td.2015.03.003

Wang, Y. M., Dong, D. Z., Cheng, X. Z., Huang, J. L., Wang, S. F., and Wang, S. Q. (2014). Electric Property Evidences of the Carbonfication of Organic Matters Inmarine Shales and its Geologic Significance: A Case of the Lower Cambrian Qiongzhusi Shale in Southern Sichuan Basin. *Nat. Gas Industry* 34 (8), 1–7. doi:10.3787/j.issn.1000-0976.2014.08.001

Weng, X., Kresse, O., and Cohen, C. E. (2011). Modeling of Hydraulic-Fracture-Network Propagation in a Naturally Fractured Formation. *SPE Prod. Operations* 26 (4), 368–380. doi:10.2118/140253-pa

Willis, R. J., and Wallroth, T. (1995). Approaches to the Modelling of HDR Reservoirs:A Review. *Geothermics* 24 (3), 307–332. doi:10.1016/0375-6505(95)00011-E

Wu, C. J., Zhang, M. F., Ma, W. Y., Liu, Y., Xiong, D. M., Sun, L. N., et al. (2014). Organic Matter Characteristic and Sedimentary Environment of the Lower Cambrian Niutitang Shale in southeastern Chongqing. *Nat. Gas Geosci.* 25 (8), 1267–1274. doi:10.11764/j.issn.1672-1926.2014.08.1267

Wu, Y. Y., Wu, S. H., and Cai, Z. Q. (2005). *Oil Field Geology*. Beijing: Petroleum Industry Press.

Xie, J. T., Fu, X. P., Qin, Q. R., and Li, H. (2021). Prediction of Fracture Distribution and Evaluation of Shale Gas Preservation Conditions in Longmaxi Formation in Dongxi Area. *Coal Geology&Exploration* 49 (6), 35–45. doi:10.3969/j.issn.1001-1986.2021.06.004

Xu, Y. F., Zuo, Y. J., Wu, Z. H., and Sun, W. J. B. (2017). Numerical Simulation of Tectonic Stress Field and Fracture Prediction of Yanshan Period in Fenggang Area. *Coal Technol.* 36 (7), 128–130. doi:10.13301/j.cnki.ct.2017.07.050

Xu, W. S. (2009). Comprehensive Study on Carbonate Reservoirs by Hydrothermal Transformation. *Inner Mongolia Petrochemical Techn.* 35 (1), 20–22. doi:10.3969/j.issn.1006-7981.2009.01.009

Yang, C. M., Bai, Y. Q., Zhu, L. W., Liu, M., and Li, Z. L. (2016). The Study of the Relationship between Development Shale Micro-feature and its Gas Production in Longmaxi Formation. *Sci. Techn. Eng.* 16 (20), 108–113. doi:10.3969/j.issn.1671-1815.2016.20.018

Yang, F., Ning, Z. F., Hu, C. P., Wang, B., Peng, K., and Liu, H. Q. (2013). Characterization Ofmicroscopic Pore Structures in Shale Reservoirs. *Acta Petrolei Sinica* 34 (2), 301–311. doi:10.7623/syxb201302012

Yang, Y. J., Lin, L., Zhang, Y. G., Ma, L. Y., and Li, D. L. (2009). Analysis on Lithological Characteristics and Sedimentary Environment of Niutitang Formation in Songlin Area, Zunyi. *Mar. Geology. Lett.* 25 (11), 21–26. doi:10.3969/j.issn.1009-2722.2009.11.004

Zhao, W., Jing, T., Xiong, X., Wu, B., and Zhou, Y. (2018). Graphitization Characteristics of Organic Matters in Marine-Facies Shales. *Geol. Sci. Technol. Info.* 37 (2), 183–191 doi:10.19509/j.cnki.dzkq.2018.0225

Ye, Y. H., Liu, S. G., Sun, W., Ran, B., Yang, D., Wang, S. Y., et al. (2012). Micropore Characteristics of Upper Sinian-Lower Silurian Black Shale in Upper Yangze Area of China. *J. Chengdu Univ. Techn. (Science& Techn. Edition)* 39 (6), 575–582.

Yu, B. S., Li, J., Zeng, Q. N., Sun, M. D., and Shi, M. (2016). *Sedimentary Environment and Diagenesis of Enriched Organic Shale*. Shanghai: East China University of Science and Technology Press, 172–175.

Yu, Y. F. (2013). *Multi-scale Structure Description and Borehole Instability Mechanism of Organic Rich Shale* (Xindu District, Chengdu, Sichuan, China: Southwest Petroleum University). Ph. D thesis.

Yuan, H., Xiao, J. F., He, X. Q., and Bai, P. (2007). Geochemical Characteristics and Formation Environment of the Niutitang Formation in the North Guizhou. *Guizhou Geology*. 24 (1), 55–59. doi:10.3969/j.issn.1000-5943.2007.01.011

Yuan, Y. S., Zhou, Y., Qiu, D. F., and Wang, Q. Q. (2015). Evolutionary Patterns of Non-tectonic Fractures in Shale during Burial. *Oil Gas Geology*. 36 (5), 822–827. doi:10.11743/ogg20150514

Yuan, Y. S., Zhou, Y., Qiu, D. F., and Wang, Q. Q. (2016). Formation Mechanism and Characteristics of Non-tectonic Fractures in Shales. *Geoscience* 1, 155–162. doi:10.3969/j.issn.1000-8527.2016.01.017

Zeng, L. B., and Li, Y. G. (2010). Tectonic Fracture in Tight Gas Sandstones of the Upper Triassic Xujiahe Formation in the Western Sichuang Basin, China. *Acta Geol. Sinica(English Edition)* 84 (5), 1229–1238. doi:10.1111/j.1755-6724.2010.00293.x

Zeng, L. B., Qi, J. F., and Wang, Y. X. (2007). Origin Type of Tectonic Fractures and Geological Conditionsin Low-Permeability Reservoirs. *Acta Geologica Sinica* 28 (4), 52–56. doi:10.3321/j.issn:0253-2697.2007.04.010

Zeng, L., Lyu, W., Li, J., Zhu, L., Weng, J., Yue, F., et al. (2016). Natural Fractures and Their Influence on Shale Gas Enrichment in Sichuan basin, china. *J. Nat. Gas Sci. Eng.* 30, 1–9. doi:10.1016/j.jngse.2015.11.048

Zeng, W. T., Ding, W. L., Zhang, J. C., Li, Y. X., Lin, T., Wang, R. Y., et al. (2016). Research on the Fracture Effectiveness of the Lower Cambrian Niutitang Shale in the southeastern Chongqing and Northern Guizhou Areas. *Earth Sci. Front.* 23 (1), 096–106.

Zhang, C. C., Wang, Y. M., Dong, D. Z., Li, X. J., and Guan, Q. Z. (2016a). Evaluation of the Wufeng-Longmaxi Shale Brittleness and Prediction of "sweet Spot Layers" in the Sichuan Basin. *Nat. Gas Industry* 36 (9), 51–60. doi:10.3787/j.issn.1000-0976.2016.09.006

Zhang, J. C., Jin, Z. J., and Yuan, M. S. (2004). Reservoiring Mechanism of Shale Gas and its Distribution. *Nat. Gas Industry* 24 (7), 15–18.

Zhang, Q., Liu, C., Mei, X. H., and Qiao, L. J. Y. (2015). Status and prospect of Research on Microscopic Shale Gas Reservoir Space. *Oil &Gas Geology.* 36 (4), 666–674.

Zhang, Q., Zhu, X. M., Li, C. X., Qiao, L. J. Y., Liu, C., Mei, X. H., et al. (2016b). Classification and Quantitative Characterization of Microscopic Pores in Organic-Richshale of the Shahejie Formation in the Zhanhua Sag, Bohai Bay Basin. *Oil &Gas Geology*. 37 (3), 422–432. doi:10.11743/ogg20150417

Zhang, S. W., Meng, Z. Y., Guo, Z. F., Zhang, M. Y., and Han, C. Y. (2014). Characteristics and Major Controlling Factors of Shale Reservoirsin the

Longmaxi Fm, Fuling Area, Sichuan Basin. *Nat. Gas Industry* 34 (12), 16–24. doi:10.3787/j.issn.1000-0976.2014.12.002

Zhao, Y. L., Yang, R. J., Yang, X. L., and Mao, Y. Q. (2006). Globular Sponge Fossils Fram the Lower Cambrian in Songlin Guizhou Province China. *Geol. J. China Universities* 12 (1), 106–110. doi:10.3969/j.issn.1006-7493.2006.01.012

Zhong, G. Y., Zhang, X. L., and Yang, Z. (2021). Logging Identification Method for Fractures in Tight sandstone Reservoirs of Yanchang Formation in Dingbian-Zhidan Area, Ordos Basin. *Prog. Geophys.* 36 (04), 1669–1675. doi:10.6038/pg2021EE0318

Zhou, W. D., Wang, Y., Bao, Z. Y., and Han, X. T. (2015). The Application of Iso-Therm Adsorption in Measuring the Shale Pore Structure. *Bull. Sci. Techn.* 31 (1), 12–18. doi:10.3969/j.issn.1001-7119.2015.01.004

Zou, C. N., Dong, D. Z., Wang, S. J., Li, J. Z., Li, X. J., Wang, Y. M., et al. (2010). Geological Characteristics, Formation Mechanism and Resource Potential of Shale Gas in China. *Pet. Explor. Dev.* 37 (6), 641–653. doi:10.1016/S1876-3804(11)60001-3

Conflict of Interest: Author ZC was employed by the company SINOPEC Star Petroleum Company.

The remaining authors declare that the research was conducted in the absence of any commercial or financial relationships that could be construed as a potential conflict of interest.

Publisher's Note: All claims expressed in this article are solely those of the authors and do not necessarily represent those of their affiliated organizations, or those of the publisher, the editors and the reviewers. Any product that may be evaluated in this article, or claim that may be made by its manufacturer, is not guaranteed or endorsed by the publisher.